



CRN: 13758

UCK 427E Combustion

**Prof. Dr. İskender Gökalp**

31.01.2024

Term Paper

Zeynep Akkuş 110200125

Ahmet Fevzi Akargöl 110200170

Ebrar Ürenden 110200162

Samet Karaca 110200719

Sezer Koyun 110200144

Metin Bora Soydan 110200142

## **CONTENTS**

### **1. INTRODUCTION**

#### **2.1 SINGLE PARTICLE COMBUSTION**

**“Aluminum combustion in CO<sub>2</sub> -CO-N<sub>2</sub> mixtures” (Ebrar Ürenden)**

**“New experimental method for the simultaneous determination of concentration and size profiles of condensed combustion products around a burning aluminum droplet” (Ebrar Ürenden)**

**“Ignition and Combustion of Levitated Magnesium and Aluminum Particles in Carbon Dioxide” (Metin Bora Soydan)**

**“Studies on the Ignition and Burning of Levitated Aluminum Particles” (Samet Karaca)**

#### **2.2 METAL DUST COMBUSTION**

**“Experimental investigation of aluminum-air burning velocity at elevated pressure” (Ahmet Fevzi Akargöl)**

**“Freely-propagating flames in aluminum dust clouds” (Zeynep Akkuş)**

**“Stabilized flames in hybrid aluminum-methane-air mixtures” (Zeynep Akkuş)**

**“Investigation of Laminar Burning Velocity in Aluminum Particle Suspensions” (Sezer Koyun)**

### **3.FACILITY SUMMARY**

## **1. Introduction (SAMET KARACA)**

The study of combustion science plays a pivotal role in modern energy systems, as it remains the dominant process for global energy production, responsible for over 80% of the world's energy generation. Researchers have long focused on understanding the combustion characteristics of various fuels to improve efficiency and develop sustainable alternatives. Historically, gaseous and liquid fuels have been the primary focus due to their extensive use in transportation and power production. Similarly, solid fuels such as coal and biomass have played a crucial role in large-scale power generation and residential heating.

Beyond these conventional fuels, metallic fuels have gained attention as a viable energy source, offering unique combustion properties and broad applicability. Metal particles, such as aluminum, magnesium, iron, and silicon, possess high energy densities, elevated flame temperatures compared to hydrocarbon fuels, and significant radiative heat transfer characteristics, making them suitable for use in thermal energy and propulsion systems. Metals have historically been used in solid rocket propellants, where their addition increases combustion temperature and stability. In recent years, researchers have explored their potential as standalone energy carriers for applications ranging from underwater propulsion via metal-water reactions to rocket propulsion using CO<sub>2</sub> as an oxidizer on Mars.

### **Energetic Advantages and Potential Applications of Metal Fuels**

One of the key advantages of metal fuels is their high energy density, which surpasses that of traditional hydrocarbons. This makes them an ideal candidate for energy-intensive applications such as boilers, swirl-stabilized burners, aerospace propulsion, and power generation. For instance, aluminum combustion has been studied for its ability to serve as a low-carbon alternative to fossil fuels, particularly in coal-fired power plants. Similarly, iron combustion has been explored as a renewable energy carrier, with the ability to be oxidized and later regenerated in a closed-loop system.

In addition to power generation, metal fuels have significant potential in propulsion applications. For example, magnesium-fueled combustors and swirl burners have been evaluated for their stability and NO<sub>x</sub> emission characteristics, showing promise for future aerospace and industrial applications. A particularly interesting byproduct of metal-water reactions is hydrogen production, which can be used in hydrogen-based power systems, including fuel cells and hydrogen combustion engines. This makes metal fuels not only a primary energy source but also an enabler of hydrogen economy technologies.

One of the most exciting applications of metal combustion is in space exploration. Research has demonstrated that metals such as aluminum and magnesium can be used as fuels for in-situ resource utilization (ISRU) on Mars, leveraging the 95% CO<sub>2</sub>-rich Martian atmosphere as an oxidizer. This approach, known as metal-CO<sub>2</sub> propulsion, has been extensively studied by Shafirovich and Varma, who demonstrated the feasibility of burning metal fuels directly with Martian CO<sub>2</sub> to generate thrust. This system could significantly reduce mission costs and payload constraints by eliminating the need for Earth-supplied oxidizers, making it a key technology for Mars ascent vehicles, landers, and robotic exploration.

Revision: Adding of Regolith Regolith after presentation

Another most exciting application of metal combustion is on the Moon. The fine, highly reactive dust layer covering the Moon's surface, known as lunar regolith, is rich in metal oxides and pure metallic particles. Elements such as iron (Fe), titanium (Ti), and aluminum (Al) present in the regolith can undergo exothermic oxidation reactions under suitable conditions, releasing significant amounts of energy. This characteristic, combined with metal particle combustion processes, presents a valuable potential for energy production and propulsion systems on the lunar surface. The combustion mechanism of regolith differs from conventional solid-fuel combustion due to the absence of atmospheric oxygen. Instead, oxidation can occur using locally extracted oxygen obtained from chemical processing of regolith or oxidizers transported from Earth. In particular, thermal plasma methods or laser-induced reactions can trigger oxidation of metal particles within the regolith at high temperatures, leading to a controlled energy release. This concept is particularly important for long-duration lunar missions, as it offers a sustainable alternative to chemical propellants and energy sources brought from Earth. Future lunar operations are expected to integrate in-situ resource utilization (ISRU) strategies to maximize efficiency and sustainability. Metals extracted from regolith can be used in controlled combustion processes to generate thermal and electrical energy for various applications, including power generation for lunar bases. Additionally, metal dust oxidation can be harnessed for propulsion systems, enabling thrusters or engines to operate using lunar-derived fuels. Furthermore, the oxidized compounds produced during combustion could serve as ceramic-like materials for constructing lunar habitats and infrastructure, reducing reliance on Earth-supplied materials. Research on the combustion potential of lunar regolith suggests that it could serve as a critical energy source for future lunar mining and colonization efforts. By utilizing locally available resources, these technologies could significantly reduce mission costs and logistical challenges associated with transporting fuel and construction materials from Earth. In the long term, harnessing the energetic potential of the lunar regolith could play a key role in establishing a sustainable space economy and enabling human presence on the Moon and beyond.

Apart from space propulsion, metal fuels have also been investigated for underwater propulsion. Since oxygen is scarce in submerged environments, metals like aluminum and magnesium can react with water to generate energy. This capability makes them an ideal energy source for torpedoes, autonomous underwater vehicles (AUVs), and long-range submarines. Unlike traditional propulsion systems, which rely on external oxidizers, metal-based propulsion offers self-sustaining, high-energy output with extended endurance.

### **Challenges in Metal Combustion**

While metal fuels offer numerous advantages, their combustion processes are significantly more complex than those of gaseous or liquid fuels. Traditional combustion models, which are typically designed for premixed or diffusion flames, cannot be directly applied to metal dust flames due to their multi-phase nature. In a metal dust flame, combustion occurs in a discrete particle system, making flame propagation highly dependent on particle size, oxidation kinetics, and radiative heat transfer effects. The presence of high-temperature condensed-phase reactants and products further complicates the modeling process, as radiation heat transfer plays a dominant role in flame stability and propagation.

Furthermore, metal combustion experiments generally fall into two major categories: single-particle combustion and metal dust flames, each of which presents unique experimental challenges.

For single-particle combustion, one of the biggest difficulties is generating and igniting individual metal particles, especially at extremely low densities. Unlike gaseous fuels, which can be easily injected into a combustion chamber, maintaining a stable supply of metal particles requires specialized particle generators. Additionally, metal particles often have high ignition temperatures, requiring precisely controlled ignition sources for reliable experiments. Another challenge lies in measuring the combustion characteristics of these particles. Due to their small size, burning metal particles undergo rapid changes in brightness and temperature, making it difficult to obtain accurate size and temperature measurements.

For metal dust flames, the experimental setup is equally complex. Achieving a uniformly dispersed metal dust cloud with a constant particle density requires sophisticated dust injection systems and specially designed burners. Moreover, metal dust flames tend to be optically thick, meaning that multiple scattering effects introduce significant challenges for optical diagnostics. Despite these difficulties, researchers have developed innovative experimental setups and applied advanced online and offline diagnostic methods to improve our understanding of metal combustion.

Figure 1 provides an overview of previous experimental studies on metal combustion, categorizing research based on metal type and combustion method. The figure reveals that aluminum is the most extensively studied metal, followed by boron and iron, due to their widespread use in energetic applications such as propellants and explosives. The chart also highlights that single-particle combustion has been studied more frequently than metal dust flames, primarily because achieving a stable dust flame is experimentally more challenging. Furthermore, the breakdown of studies shows that aluminum predominantly burns in the vapor phase, while iron combustion is typically heterogeneous. These insights underscore current research trends and help guide the development of future experimental approaches.

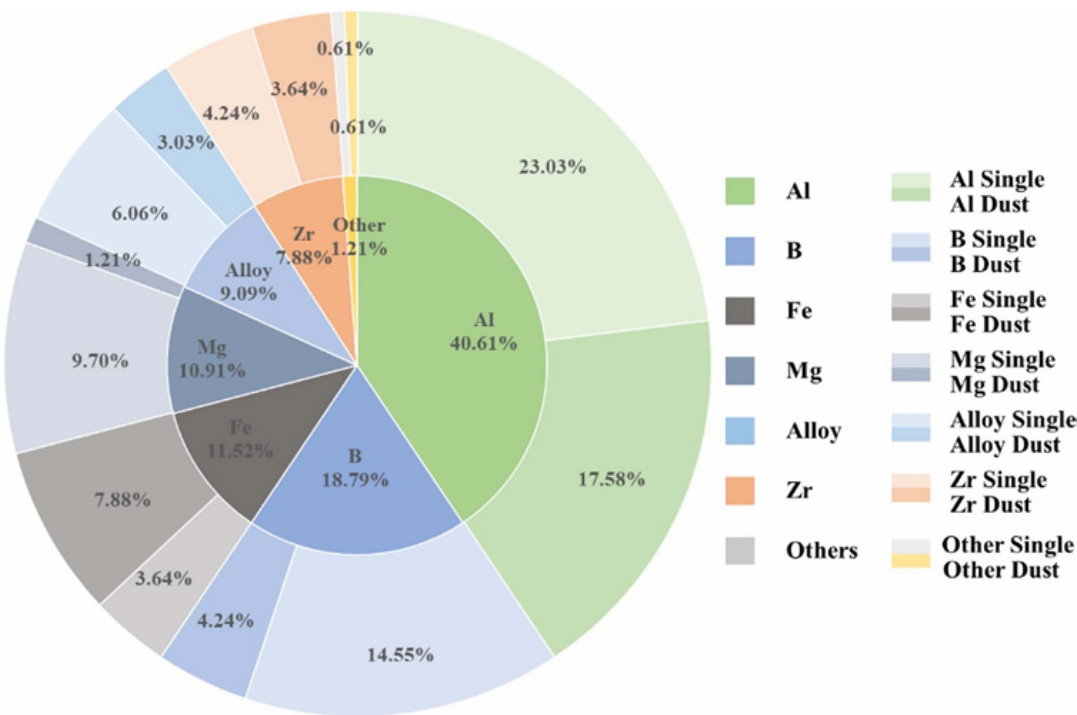


Figure 1: Statistics of the previous experimental studies on metal combustion [1]

## Future Directions in Metal Combustion Research

With ongoing advancements in combustion diagnostics, metal fuel recycling, and hybrid energy applications, metal fuels are poised to play a transformative role in future propulsion and power generation technologies. Their potential applications span space exploration, terrestrial energy storage, high-efficiency industrial power systems, and underwater propulsion. As research continues to refine combustion models, diagnostic methods, and fuel regeneration processes, metal combustion is expected to become a key component in the transition toward high-efficiency, zero-carbon energy solutions.

By addressing the fundamental challenges of metal combustion, developing new experimental methodologies, and exploring novel applications, metal fuels have the potential to revolutionize global energy infrastructure. Whether in aerospace, defense, power generation, or advanced manufacturing, metal combustion stands as a promising alternative to traditional hydrocarbon-based energy systems, paving the way for a more sustainable and energy-efficient future.

## Sample Facilities

Several facilities worldwide have been established to study solid particle combustion under various conditions. These facilities provide advanced experimental setups and diagnostic tools that have significantly contributed to the understanding of solid particle combustion behavior. The following examples highlight the capabilities and technologies employed by some of these facilities:

**JAXA's Solid Combustion Experiment Module (SCEM):** The Solid Combustion Experiment Module (SCEM), developed by the Japan Aerospace Exploration Agency (JAXA), is designed to investigate the combustion properties of solid fuels in microgravity. SCEM is installed in the Japanese

Experiment Module (JEM) "Kibo" onboard the International Space Station (ISS). This facility enables the study of combustion phenomena in the absence of gravitational effects, providing insights into flame behavior, ignition mechanisms, and combustion efficiency under microgravity conditions.

(Source: [JAXA SCFM](#))

**Sandia National Laboratories (USA):** Sandia National Laboratories specializes in advanced optical diagnostic equipment and multipurpose laser systems for combustion studies. These tools allow for high-resolution imaging and precise measurements of flame dynamics, particle interactions, and temperature distributions. Sandia's facilities are particularly known for their contributions to engine combustion research and the development of innovative diagnostic techniques.

(Source: [Sandia National Laboratories](#))

**ICARE CNRS (France):** The ICARE Laboratory of the CNRS (Centre National de la Recherche Scientifique) in France focuses on solid particle combustion using cutting-edge technologies such as electrodynamic levitation devices and multispectral light attenuation systems. These systems enable precise control and analysis of particle behavior during combustion, offering valuable insights into reaction mechanisms and flame characteristics.

**DLR (Germany):** The German Aerospace Center (DLR) operates high-pressure and high-temperature combustion chambers for the study of particle-laden flames. These facilities simulate extreme conditions, enabling researchers to investigate combustion processes at elevated pressures and temperatures, which are representative of real-world propulsion and industrial systems.

**Beijing Institute of Technology (China):** The Beijing Institute of Technology is equipped with advanced spectroscopic tools and gas analyzers to study metal particle combustion. These technologies allow detailed chemical analysis and monitoring of combustion gases, enhancing the understanding of reaction kinetics and emission characteristics during metal particle combustion.

This term paper reviews and compares multiple studies on metal particle combustion and aluminum dust flames to evaluate their experimental methodologies and findings. Several key papers were examined for their contributions to the field. For dust combustion, the reviewed works include "*Experimental Investigation of Aluminum-Air Burning Velocity at Elevated Pressure*" by Ahmet, "*Freely-Propagating Flames in Aluminum Dust Clouds*" and "*Stabilized Flames in Hybrid Aluminum-Methane-Air Mixtures*" by Zeynep, and "*Investigation of Laminar Burning Velocity in Aluminum Particle Suspensions*" by Sezer. For particle combustion, this study examines "*Aluminum Combustion in CO<sub>2</sub>-CO-N<sub>2</sub> Mixtures*" and "*New Experimental Method for the Simultaneous Determination of Concentration and Size Profiles of Condensed Combustion Products Around a Burning Aluminum Droplet*" by Ebrar, "*Ignition and Combustion of Levitated Magnesium and Aluminum Particles in Carbon Dioxide*" by Bora, and "*Studies on the Ignition and Burning of Levitated Aluminum Particles*" by Samet.

## 2.1 Single Particle Combustion (EBRAR ÜRENDE)

This study investigates the single-particle combustion of aluminum droplets by characterizing the concentration and size distributions of condensed alumina particles formed during combustion. The aim is to understand the combustion processes of high-energy-density particles, such as aluminum, which are commonly used as propellants in space and defense applications. The research analyzes

parameters such as particle size, combustion rate, oxidizer type, and temperature on combustion dynamics. Furthermore, the study validates mathematical and numerical models with experimental data to predict the behavior of oxides formed during combustion.

### **"Aluminum Combustion in CO<sub>2</sub>-CO-N<sub>2</sub> Mixtures" (2021)**

This study investigates the combustion behavior of aluminum particles in different gas mixtures, specifically CO<sub>2</sub>, CO, and N<sub>2</sub>. While aluminum combustion in oxygen is well-documented, its reaction with less-studied oxidizers such as CO<sub>2</sub> and CO remains less explored. This research aims to characterize the combustion mechanisms in these environments and analyze how different oxidizers influence combustion duration and reaction dynamics.

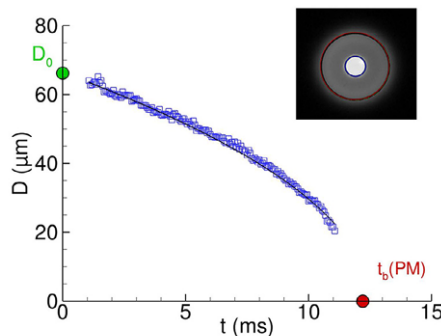


*Figure 2. Typical diameter evolution  $D(t)$  obtained from direct imaging*

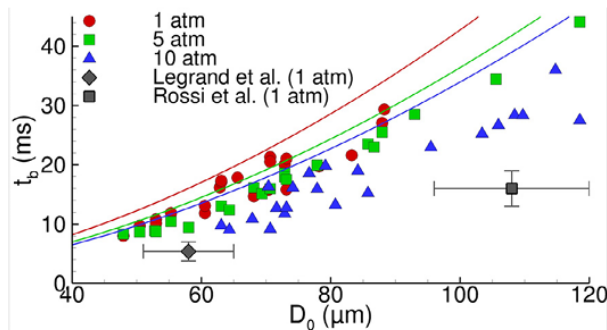


*Figure 3. Measured burning time  $t_b$  with particle size  $D_0$  and pressure*

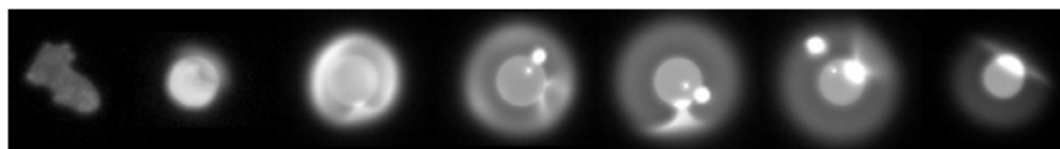


*Figure 4. Typical combustion sequence in pure CO*

#### **The experimental setup:**

1. **Electrodynamic Levitator** – Used to suspend a single aluminum particle in the gas mixture, ensuring an isolated combustion environment.

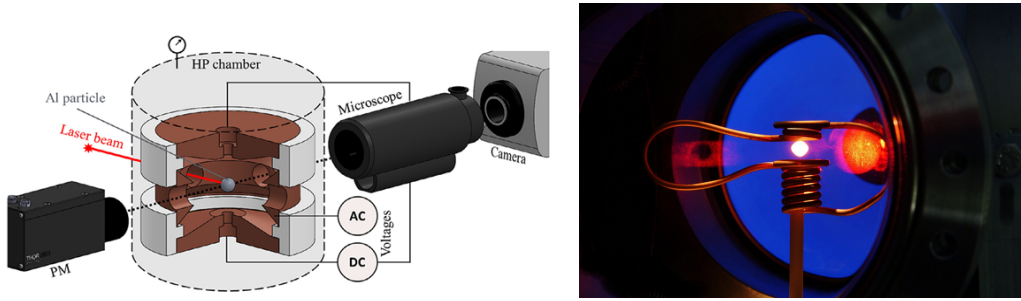


*Figure 5. Schematic representations of the electrodynamic levitator*

2. **High-Speed Camera** – Captured high-resolution, high-frequency images of the burning aluminum particle.
3. **Photomultiplier Tubes (PMTs)** – Monitored light emission to determine combustion duration.
4. **Heating System** – A system to modify the experimental setup for handling steam ( $H_2O$ ).
5. **Steam Supply System** – Recently added for future experiments involving  $H_2O/CO_2$  and  $H_2O/O_2$  mixtures.
6. **Controlled Gas Mixture Chamber** – Allowed precise control of gas compositions ( $CO_2$ ,  $CO$ ,  $N_2$ , and future  $H_2O$  mixtures).
7. **Pressure Regulation System** – Maintained stable experimental conditions, enabling studies at pressures up to at least 15 atm.

## Results and Discussion

### Combustion in Different Gas Environments:

**$CO_2$  Atmosphere:** Combustion followed a diffusion-controlled mechanism, where the burning rate was dependent on particle diameter.

**$CO$  Atmosphere:** A chemically limited heterogeneous reaction was observed. Unlike in  $CO_2$ , no diffusion flame was formed, and combustion was prematurely terminated.

**$CO_2$ - $CO$  Mixtures:** As the  $CO$  concentration increased, combustion duration extended. This suggests that  $CO$  has a weaker oxidizing effect compared to  $CO_2$ , leading to a slower reaction rate.

### Observations

**Combustion Duration ( $t_b$ ):** Estimated primarily through PMT signals, which directly measured light emission from burning particles.

**Particle Diameter Evolution ( $D(t)$ ):** One of the key innovations of this experimental setup was the ability to monitor real-time diameter changes with high precision using automated image processing. This provided new insights into the combustion dynamics that were not previously accessible using only light emission measurements.

**"New experimental method for simultaneous determination of concentration and size profiles of condensed combustion products around a burning aluminum droplet" (2024)**

The aim of this experiment is to investigate the combustion dynamics of aluminum droplets by characterizing the size and concentration distributions of the condensed alumina particles formed during combustion. The experimental setup focuses on understanding the combustion behavior of high-energy-density aluminum particles, which are often used as propellants in space and defense applications. The experiment intends to explore the effects of particle size, combustion rate, and environmental conditions (oxidizer type, temperature, and pressure) on the combustion process. Additionally, the study aims to provide experimental data for validating computational models predicting oxide formation during combustion.

**Experimental Setup and Equipment:**

The experiment utilizes an electrodynamic levitator to hold a single aluminum particle, isolating the combustion process from convective effects. The particle is ignited using a CO<sub>2</sub> laser, providing symmetrical heating. The combustion process occurs in a test chamber, where parameters like temperature, pressure, and oxidizer concentration are controlled.

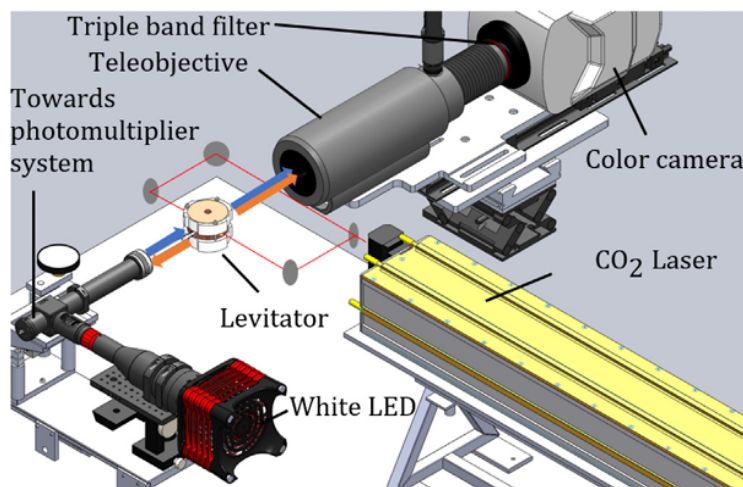


*Figure 6. Schematic of the full experimental setup, including the pathways of the CO<sub>2</sub> laser beam (red line), the LED light (blue arrows), and the combustion emissions (orange arrows)*

Key equipment used includes:

**1. Phantom T-2410 High-Speed Color Camera:**

- Measures light intensity at three different wavelengths (450 nm, 530 nm, and 630 nm) using RGB matrices.
- Operates at high speeds (4 kHz to 18 kHz), capturing frames in as short as 0.25 ms.
- Although capable of a maximum speed of 78 kHz, it was operated at lower speeds during the experiment due to reduced light levels caused by the triple-band filter.

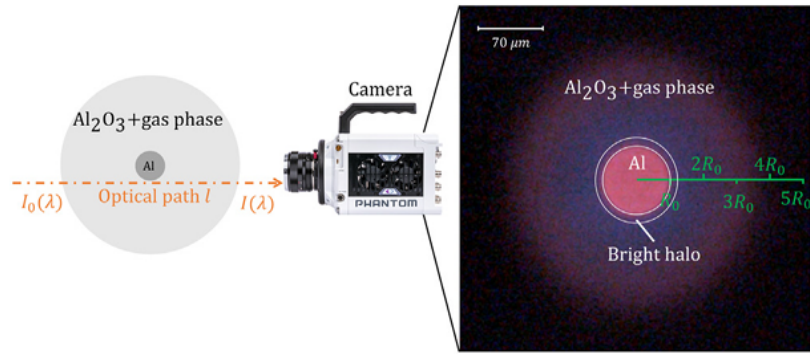


*Figure 7. The left part of the figure is a schematic of a light ray of intensity  $I_0$  passing through the oxide smoke of the burning particle along the optical path of length  $l$  and reaching the camera sensor with an intensity  $I$ . The right part of the figure is an example of image obtained for a particle burning in air at atmospheric pressure*

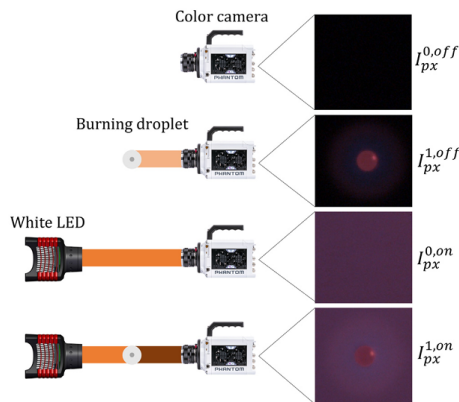


*Figure 8. Schematic of the four intensities required to calculate the integrated optical depth of the alumina*

2. **Questar QM 100 Teleobjective Lens:**
  - Captures high-resolution, symmetric, and detailed images.
  - Analyzes the size and concentration profiles of nano-scale alumina particles.
  - Measures light intensity across multiple wavelengths to examine the spectral properties of the particles.
  - Minimizes interference from flame emissions to isolate light absorbed solely by the particles.
3. **White LED (SOLIS-3C):** Used as backlighting to measure light absorption by alumina particles at various wavelengths.
4. **Multispectral Light Attenuation Method:** Measures the light intensity at the wavelengths mentioned above, providing information on particle size distribution and concentration.
5. **Horiba PG-250 Gas Analyzer and Kistler 601A Pressure Sensors:** Monitor gas composition and pressure during combustion, providing additional data on combustion dynamics.

## **Experimental Results:**

The analysis revealed that smaller alumina particles (~75 nm) were formed in the reaction zone, while larger particles (~86 nm) were observed in the surrounding region. This information is critical for understanding the combustion dynamics of aluminum particles and provides insights into particle formation and growth. The findings suggest that the formation of the oxide layer influences the combustion rate and the size distribution of the particles.

## **Experimental Equipment Used:**

- **Electrodynamic Levitation Device:** Holds aluminum particles in place during combustion.
- **CO<sub>2</sub> Laser:** Ignites the particle and provides symmetric heating.
- **High-Speed Camera:** Captures rapid changes in the combustion process.
- **Multispectral Light Attenuation System:** Measures particle size and concentration.
- **Gas Analyzers:** Monitors combustion byproducts and environmental conditions.

## ***“Studies on the Ignition and Burning of Levitated Aluminum Particles” (SAMET KARACA)***

A high-pressure experimental setup has been designed to study the combustion of levitated aluminum particles ignited by a CO<sub>2</sub> laser in air. The electrodynamic levitator ensures sufficient residence time for observing the complete burning process under both normal and high-pressure conditions. These experiments enable the measurement of ignition delay and burning duration of aluminum particles. The particle initial equivalent diameters are estimated to vary from 35 nm to 70 nm. Additionally, the collected data, along with high-speed imaging, provide valuable insights into the combustion behavior of aluminum particles across different conditions.

## **Experimental Setup**

The single particle burning system comprises the following:

**1.High-Pressure Combustion Chamber:** The combustion chamber is designed to create a controlled high-pressure environment that closely replicates conditions found in solid rocket motors, thereby ensuring the relevance of experimental data. Constructed from an aluminum alloy to withstand pressures up to 8 MPa, it measures 100 mm in diameter and 200 mm in length—dimensions chosen to accommodate both the electrodynamic levitator and the necessary optical systems.

**2.Electrodynamic Levitator:** The levitator isolates single aluminum particles, ranging from 20 to 100 μm in diameter, to prevent interference from physical supports and neighboring particles, allowing for a more representative observation of free particle burning. It utilizes top and bottom electrodes, each 80 mm in diameter, to generate an electric force opposing gravity for vertical stabilization. Additionally, a ring electrode with AC voltage provides both lateral and vertical forces, ensuring precise positioning and stabilizing the particle within the chamber. This design eliminates extraneous factors that could distort the combustion process, facilitating accurate analysis of particle behavior.

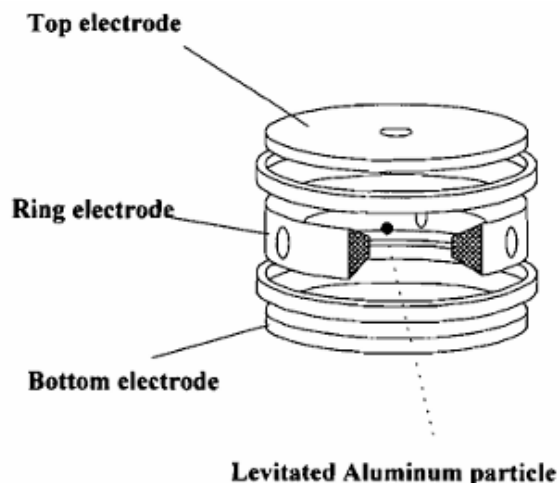


*Figure 9. A schematic of the electrodynamic levitator used to isolate a single aluminum particle*

**3.CO<sub>2</sub> Laser Ignition System:** A 20 W CO<sub>2</sub> laser provides a consistent and controlled ignition source for the aluminum particles, ensuring reproducible combustion events. By maintaining a symmetric focus on the particle, the system avoids displacement caused by thermophoretic forces, thereby guaranteeing uniform heating and reliable ignition. Chosen for its precision and non-contact nature, the CO<sub>2</sub> laser introduces minimal disturbance to the particle and is particularly well-suited for experiments requiring high accuracy in both temperature and positioning.

**4.Optical Diagnostics:** To capture detailed combustion dynamics, two types of images are captured during the experiment. A high-speed video camera (Kodak Ektapro 1000) records the entire burning process at a rate of one frame per millisecond. Additionally, a conventional CCD video camera with an electronic shutter captures a single image of the burning particle at an exposure time of 1/4000 s. Photomultiplier tubes (Hamamatsu R2752) equipped with interference filters at 488 nm and 514.5 nm enable brightness measurements and two-color pyrometry, facilitating accurate temperature and combustion phase analysis. The signals from the photomultipliers and the laser pulse trigger are recorded on a PC using a DAS-50 acquisition card operating at a sampling rate of 100 kHz. A mirror is used to reflect the laser beam, ensuring symmetric irradiation of the particle and preventing displacement due to thermophoretic forces. Since the measured characteristic times are extremely short, lasting only a few milliseconds, a synchronizer is required to coordinate all devices. It ensures precise triggering of the laser, acquisition interface, and camera.

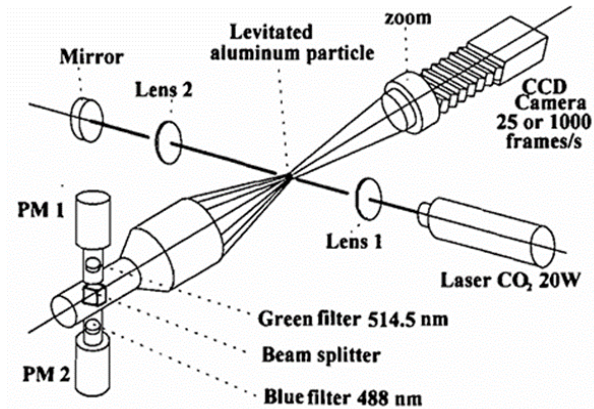


*Figure 10. Optical set-up for particle ignition and brightness time measurements*

## Measurement Results

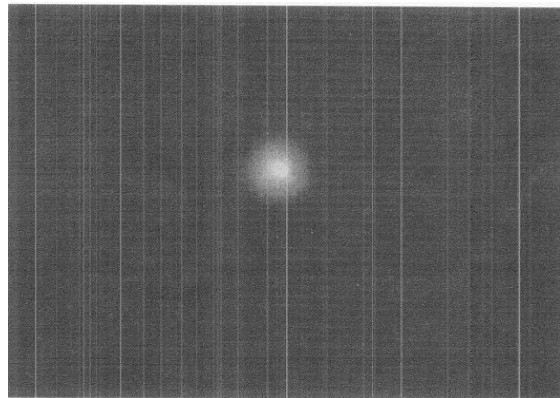
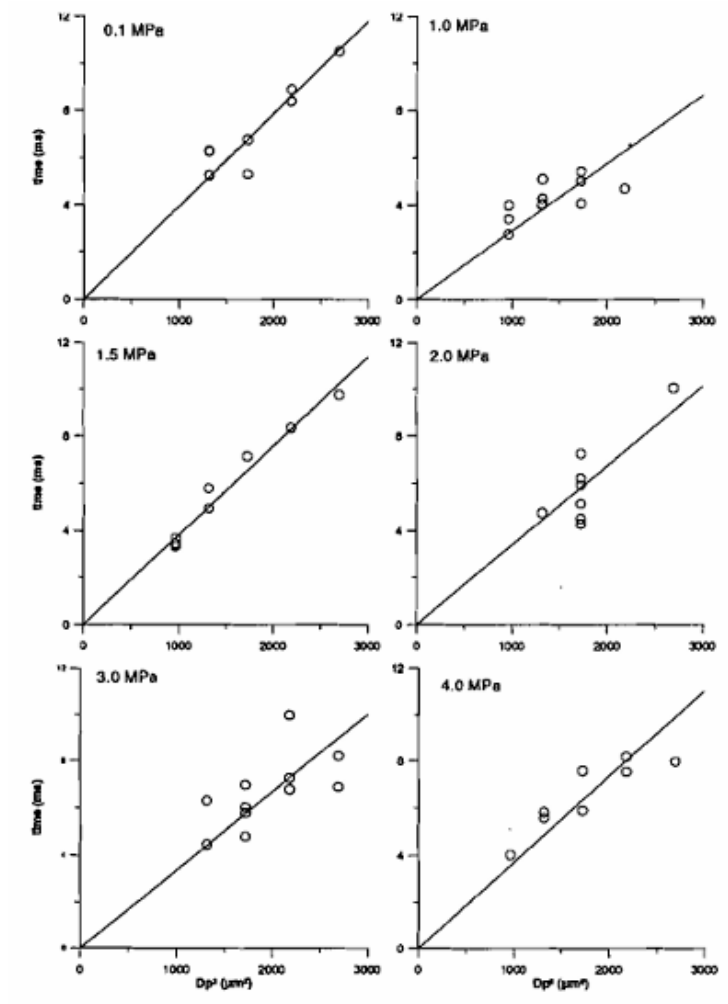


PLATE I Single aluminum particle burning in 0.10 MPa air. See COLOR PLATE III.

1. **Burning Times:** According to the referenced study, burning times decrease at lower pressures as pressure increases, then remain essentially constant above approximately 2 MPa as seen in Figure 11. The burning time appears to be proportional to  $D_p^2$ .



*Figure 11. Experimental burning times as function of initial particle diameter squared, obtained at 0.1, 1.0, 1.5, 2.0, 3.0 and 4.0 MPa air. For all these runs, the laser is turned off at ignition.*

The average burning rates gradually increase with pressure up to around 2 MPa, after which they remain constant at higher pressures as seen in Figure 12.

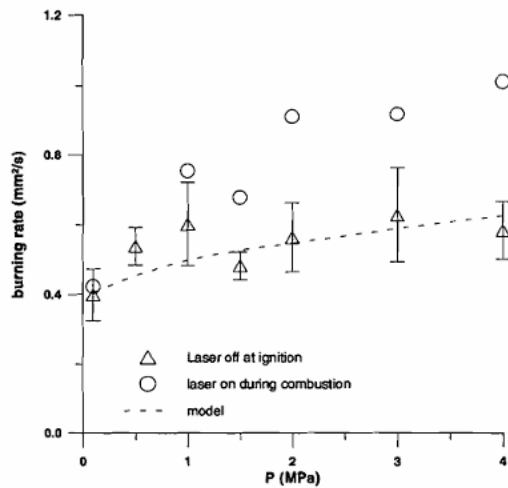


*Figure 12. Pressure Effect On the predicted and measured burning rate*

2. **Heating time or ignition delay:** Ignition delay refers to the time between the start of laser heating and the point at which the particle ignites.. In the referenced study, ignition delays were found to remain relatively constant despite changes in pressure, indicating the dominant role of particle characteristics in determining ignition behavior. Understanding ignition delay is crucial for developing propellants that ignite more quickly and reliably, particularly in time-sensitive applications like rocket launches.

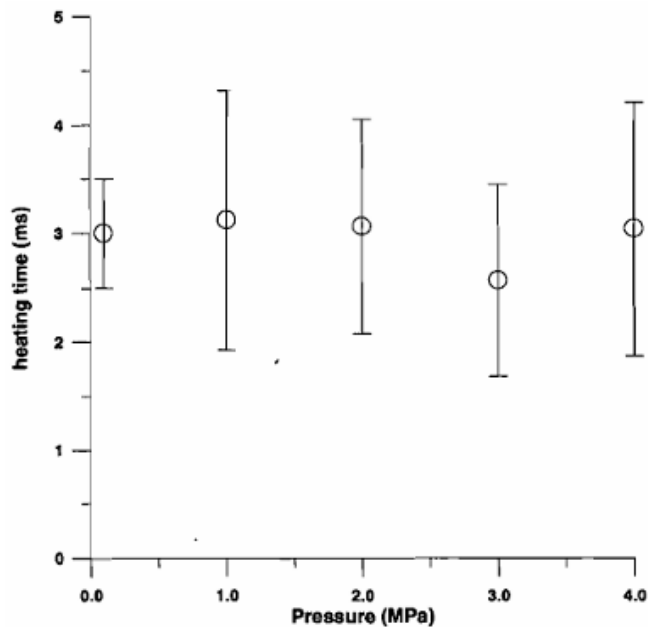


*Figure 13. Heating Time as a function of pressure in air*

## Conclusion

The single-particle burning system presented here demonstrates an effective method for investigating aluminum combustion under high-pressure conditions. Its electrodynamic levitator, combined with a CO<sub>2</sub> laser ignition source and advanced optical diagnostics, enables precise measurement of both ignition delay and burning duration. This approach reveals how factors such as particle size and ambient pressure influence overall combustion efficiency. The ignition delay remains unchanged as pressure increases, while the burning rate shows a slight increase at moderate pressures and stabilizes at higher pressures.

## ***“Ignition and Combustion of Levitated Magnesium and Aluminum Particles in Carbon Dioxide”*** **(METİN BORA SOYDAN)**

The combustion of aluminum and magnesium particles plays a pivotal role in rocket propulsion, where high energy density and rapid heat release are crucial for achieving efficient thrust. Aluminum is a key fuel additive in solid rocket propellants, contributing significantly to their performance by releasing substantial energy during combustion. Its high combustion enthalpy increases the specific

impulse of rocket motors, enabling them to achieve the extreme velocities required for space exploration and missile systems. Magnesium, with its lower ignition temperature and bright, intense flame, is often used in igniters to ensure reliable and efficient ignition of propellants under varying conditions. Aluminum particles, particularly in micron or nano-scale form, enhance the burn rate and energy output by providing a larger reactive surface area, which is essential for the rapid release of energy in propulsion systems.

The reaction of aluminum and magnesium combustion in gaseous carbon dioxide holds considerable interest for various rocket engine applications. Current solid propellants normally contain metals as high energetic fuel, and the gaseous CO<sub>2</sub>, along with H<sub>2</sub>O, is often the main oxidizing component for metal particles in a solid rocket motor (Legrand et al.). Aluminum is characterized by a higher heat of combustion than magnesium, and for this reason it is aluminum that is used in most solid rocket motors (Brooks and Beckstead, 1995). But magnesium also has superior properties such as igniting easier especially in carbon dioxide including atmospheres. To answer and investigate the questions regarding metal combustion in solid propellant rocket engines, an experimental set up will be created. During this process the article of “Ignition and Combustion of Levitated Magnesium and Aluminum Particles in Carbon Dioxide” from B. Legrand et al. will be used as a guide. This article explores the findings and methodologies outlined in the study of magnesium and aluminum particle ignition in carbon dioxide environments. Using an electrodynamic levitator and CO<sub>2</sub> laser ignition system, the experiments assess ignition delays, burning rates, and combustion residue properties under various conditions.

By following these, an experimental system was set up to investigate behavior of different size aluminum and magnesium particles in the carbon dioxide environment. We will be having a similar set up to the one used for the previous experiment above. These experiments investigate key properties such as ignition delays, burning rates, and the formation of alumina residue during combustion—factors critical to optimizing solid rocket propulsion. The referenced study, for example, aimed to examine the effects of high-pressure environments on these combustion properties. Using an electrodynamic levitator and a CO<sub>2</sub> laser ignition system, researchers were able to isolate individual particles, ignite them in controlled settings, and observe detailed combustion behaviors. This research not only enhances understanding of aluminum’s combustion mechanisms but also tackles challenges like slag accumulation in solid rocket motors, highlighting its practical applications while comparing with the combustion of magnesium. The findings contribute to the design, performance, and cost analysis of single-particle combustion systems, as discussed in this report.

## 2. System Description

### Experimental Setup

The experimental system employed consists of several key components. The High-Pressure Combustion Chamber provides a controlled high-pressure environment to replicate conditions in solid rocket motors. It is fabricated from high-strength aluminum alloy, designed to withstand pressures up to 8 MPa, with a 100 mm diameter and 200 mm length to support the electrodynamic levitator and allow optical access. The chamber includes Zn-Se and quartz windows for infrared and visible light diagnostics. The Electrodynamic Levitator isolates single particles to eliminate interference from supports or neighboring particles. It features top and bottom electrodes for vertical stabilization and a ring electrode with AC voltage for lateral stabilization, accommodating particles ranging from 20 to

100  $\mu\text{m}$  in diameter. The CO<sub>2</sub> Laser Ignition System provides a consistent, non-contact ignition source for particles. It uses a 20 W laser that focuses symmetrically on the particle to ensure even heating and reliable ignition. The Optical Diagnostics system enables high-resolution imaging and temperature analysis during combustion. High-speed video cameras and photomultiplier tubes, equipped with interference filters at 488 nm and 514.5 nm, are used for brightness and combustion phase analysis.

### **Measurement Techniques**

Several measurement techniques are employed to analyze combustion characteristics. Burning Times are determined using synchronized high-speed imaging and photomultiplier readings to measure combustion duration, providing insights into particle combustion efficiency and behavior under different pressures. Ignition Delay refers to the time from laser heating to particle ignition, highlighting the effects of particle properties and environmental conditions on reactivity. Particle Size Analysis involves measuring initial and post-combustion particle diameters using calibrated imaging tools, correlating particle size with combustion efficiency and residue formation.

## **3. Design Considerations**

### **High-Pressure Adaptation**

A robust high-pressure chamber was essential for accurate simulation of conditions in propulsion systems. The chamber's construction from aluminum alloy ensures durability and resistance to high-pressure conditions up to 8 MPa. The dimensions of the chamber, with a 100 mm diameter and 200 mm length, were optimized for housing the electrodynamic levitator and providing adequate optical access. Optical materials, such as Zn-Se and quartz, were specifically chosen to allow precise infrared and visible light transmission without distortion, enabling accurate diagnostics during combustion experiments.

### **Particle Stabilization**

The stabilization of particles during combustion is critical for obtaining reliable data. The electrodynamic levitator was designed to isolate particles ranging from 20 to 100  $\mu\text{m}$  in diameter. It achieves stabilization through top and bottom electrodes that provide vertical control, while a ring electrode with AC voltage maintains lateral stability. This design eliminates physical supports, which could interfere with the combustion process, and ensures accurate analysis of particle burning behaviors. The levitator's capability to operate under high-pressure conditions further enhances its suitability for propulsion-related research.

### **Optical and Data Acquisition**

Optical diagnostics and data acquisition systems are integral to the experimental setup. High-speed cameras capture real-time combustion dynamics with millisecond precision, providing visual data on flame propagation and particle behavior. Photomultipliers equipped with interference filters at 488 nm and 514.5 nm enable detailed brightness and temperature measurements, while two-color pyrometry ensures accurate temperature data. Synchronization between the laser ignition system and optical diagnostics is achieved using a DAS-50 acquisition card, operating at 100 kHz. This high temporal resolution allows for comprehensive analysis of rapid combustion events. Furthermore, the integration

of these systems ensures that all measurements are precise and repeatable, contributing to the reliability of the experimental findings.

## Conclusion

This study emphasizes the importance of single particle burning systems for advancing combustion research. The integration of high-pressure chambers, levitation technology, and precise optical diagnostics enables detailed analysis of combustion dynamics. The system's ability to replicate realistic propulsion environments makes it invaluable for understanding slag accumulation and optimizing the performance of solid rocket propulsion systems. Future work should explore additional materials and pressure conditions to further enhance the applicability of these findings.

This study emphasizes the importance of single particle burning systems for advancing combustion research. The integration of high-pressure chambers, levitation technology, and precise optical diagnostics enables detailed analysis of combustion dynamics. While initial costs are significant, the insights gained are crucial for improving the performance and reliability of solid rocket propulsion systems. Future work should explore additional materials and pressure conditions to further enhance the applicability of these findings.

## 2.2 METAL DUST COMBUSTION

### **“Experimental investigation of aluminum-air burning velocity at elevated pressure” (AHMET FEVZİ AKARGÖL)**

#### **Introduction**

The combustion of metal dust, particularly aluminum, has gained interest due to its high energy density, abundance, and potential application in propulsion and energy systems. Aluminum-air flames can sustain combustion under various conditions, making them valuable for industrial applications, military propellants, and alternative energy sources. However, despite extensive research on atmospheric-pressure aluminum flames, limited studies exist on their behavior at elevated pressures.

Understanding burning velocity in aluminum dust flames is crucial for determining flame stability, efficiency, and performance in practical applications. Previous studies have shown that metal dust flames exhibit unique burning characteristics, with factors such as particle size, oxidizer concentration, and turbulence significantly affecting flame propagation. However, these studies were mostly conducted at atmospheric pressure, and the impact of elevated pressure on burning velocity, interparticle interactions, and flame structure remains unclear.

This study aims to investigate the burning velocity of aluminum-air flames at elevated pressures, ranging from 1 to 7.2 bar, using an optically accessible combustion chamber. The results provide new insights into how pressure influences metal dust combustion, which is relevant for high-pressure applications such as rocket propulsion, gas turbines, and industrial combustion systems.

#### **Results and Discussion**

##### **Burning Velocity at Elevated Pressure**

Experimental results indicate that burning velocity decreases with increasing pressure. At atmospheric pressure (1 bar), the measured burning velocity for H-15 aluminum powder was approximately 10 cm/s, consistent with previous atmospheric-pressure studies. As the chamber pressure increased to 5.2 bar, burning velocity decreased by nearly 50%, and at 7.2 bar, it was significantly lower.

This trend is in agreement with prior studies on metal dust flames, which suggested that at higher pressures, the oxidizer density increases and the interparticle spacing decreases, leading to higher oxidizer competition and asymmetric heating effects on burning particles. The results suggest that as pressure increases, particles burn in a more diffusion-limited regime, reducing the overall burning velocity of the system.

When considering only laminar flow conditions, the decline in burning velocity with increasing pressure is slightly less pronounced, indicating that turbulence effects contribute to this reduction at higher pressures.

### Inter-Particle Spacing and Flame Interactions

As pressure increases, the metal dust concentration in the flame also increases, which causes a reduction in mean interparticle distance. Calculations based on the particle size distribution indicate that at 7.2 bar, the average interparticle spacing is significantly smaller than at 1 bar, leading to increased local oxidizer competition.

Flame standoff distance, which represents the separation between a burning particle and its surrounding vapor-phase flame, also decreases with increasing pressure. This results in flame merging and overlapping, which can cause a reduction in the effective burning surface area of particles, leading to further decreases in burning velocity.

Additionally, radiation heat transfer losses become more significant at higher pressures, contributing to the overall decrease in flame propagation speed. These effects are consistent with previous research showing that atmospheric-pressure aluminum flames are less influenced by radiation compared to high-pressure flames, where radiative losses can account for over 20% of the total heat release.

All experimental tests described in this work were carried out at the Cryogenic Combustion Laboratory within the Kenneth K. Kuo High Pressure Gas Lab at The Pennsylvania State University, in partnership with the Penn State Applied Research Laboratory (ARL).

### Experimental Setup:

The experimental apparatus comprises three primary components: a high-pressure metal powder feed system, a fuel injection and oxidizer mixing element (flange insert), and a high-pressure combustion chamber with optical accessibility.

Additional auxiliary systems were implemented for pressure regulation and purging of the main components. The experiment was conducted within a reinforced-concrete test cell, with system operation controlled remotely from an adjacent room.

A custom-developed National Instruments LabVIEW VI program was utilized for both system control and data acquisition, interfacing with analog/digital modules housed within a National Instruments cDAQ chassis.

This chapter provides a detailed discussion on the design of the experimental hardware, as well as the control and data acquisition systems.

### **Hardware:**

All metal components were manufactured using 316L stainless steel, chosen for its cost-effectiveness and strong mechanical properties at elevated temperatures.

When the AFV and oxidizer control valve (OFV) are opened, the fuel and oxidizer converge at the injector head, mixing as they pass through the length of the flange insert. Upon reaching the end of the flange insert, the mixture is ignited, generating a continuous, self-sustaining flame inside the combustion chamber. The flame is observed through the chamber's optical window, while reaction products exit via the exhaust line. The entire process was operated remotely, with typical test durations lasting around thirty seconds.

### **Fuel Feed System:**

For a given fuel type, the mass flow rate of the metal powder is determined by the orifice diameter and the differential pressure across it.

The system was filled with metal powder by removing the cap and pouring the powder through an ASTM 100 mesh sieve and a funnel. The fuel feed reservoir, once loaded, was secured to a fixture on the second level of the test cell, as illustrated in Figure 14.

The carrier gas, argon, was supplied from a Praxair type-T compressed gas cylinder. Its pressure was regulated at the cylinder using a 0–200 psi pressure regulator. Flow control was managed via a Swagelok ball valve.

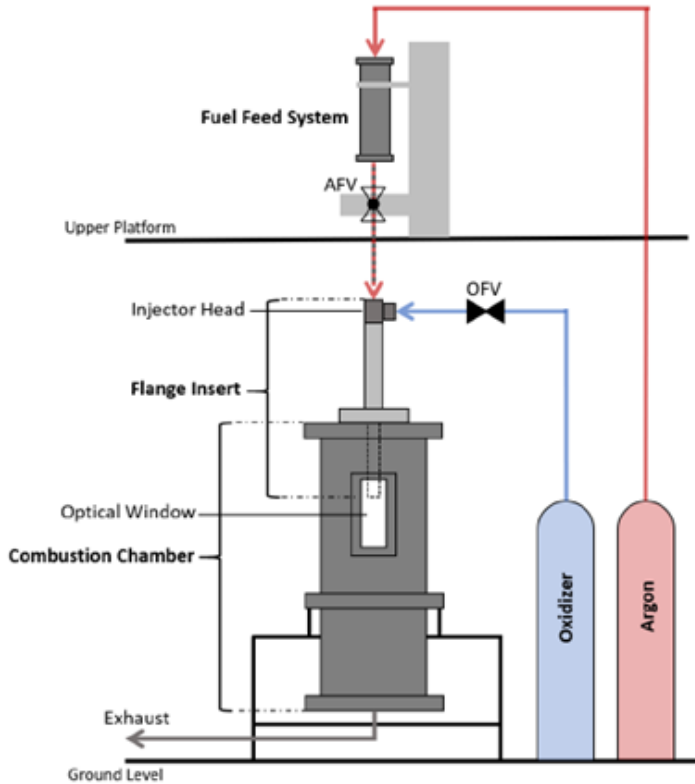


*Figure 14. Schematic of major components of the metal dust flame combustion experiment.*

### Fuel Feed Calibration

The metal powder flow rate from the fuel feed system was not measured directly during testing. Instead, it was determined through experimental calibration, establishing a correlation between the powder flow rate and the differential pressure across the fuel feed system for a given orifice diameter.

During hot-fire testing, the same differential pressure was recorded, allowing the metal powder mass flow rate to be estimated using the previously generated calibration curve.

For each calibration point, the fuel feed system was pressurized with argon to a pressure ranging between 3 and 10 psi.

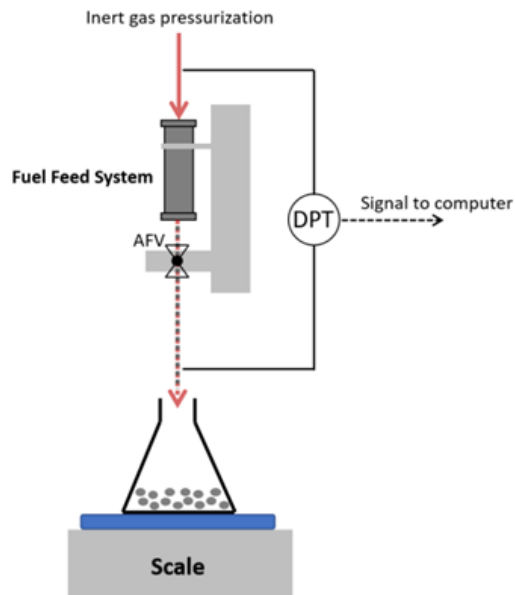


Figure 15. Experimental configuration for fuel feed system calibration

H10 Al Powder – 0.0095" orifice		
Time (s)	Mass Al (g)	
0	-	
5	0.6	$\Delta$ Mass (g)
15	2.4	$>1.8$
25	4.3	$>1.9$
35	6.1	$>1.8$

Average =  $1.83\text{g} \div 10\text{s} = 0.183\text{g/s}$

Figure 16. Example fuel feed system calibration calculation

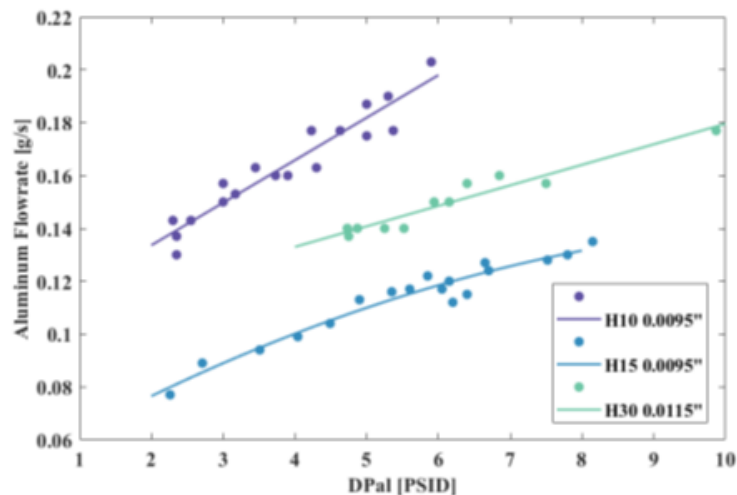


Figure 17. Fuel feed system calibration curves for H-10, H-15, and H-30 aluminum powders. Orifice diameter included next to powder size in legend.

## Ignition System

The ignition system comprises two 20 AWG copper wires, a 30 AWG nickel-chromium (nichrome) hotwire, and a solid propellant igniter. The igniters were fabricated using an aluminized composite solid propellant.

A 2-wire Conax compression fitting was used as the igniter feed-through, providing a high-pressure seal that allowed the copper wires to pass through the flange insert body.

On the exterior of the chamber, at the top of the flange insert body, two leads were available for connecting the copper wires to a variable transformer (Variac). Inside the chamber, at the bottom of the flange insert, the copper wires were electrically shielded by ceramic tubes and guided to the lower section of the mixing tube. Near the bottom, the ceramic shielding ended, exposing the copper wires, which were then connected to the nichrome wire.

One drawback of this ignition method is that the igniter must be replaced after each test.

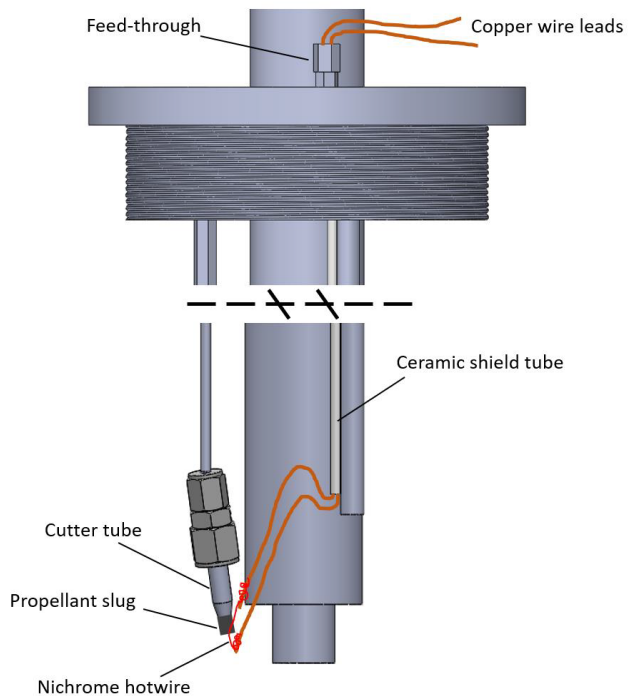


Figure 18. CAD model image of ignition system elements on flange insert outer tube/body with 0.75" mixing tube.

The igniters used in this experiment, shown in Fig. 18, were all fabricated from the same composite solid propellant. This propellant consisted of hydroxyl-terminated polybutadiene, ammonium perchlorate, aluminum, and ferric oxide. The material was sourced from prior research conducted at the High Pressure Combustion Laboratory.

Development testing was required to determine the appropriate size of the "cutter tube" and the optimal length of the propellant slug for effective ignition.

## Combustion Chamber

The combustion chamber, depicted in Fig. 19, is a high-pressure vessel made of optically accessible 304 stainless steel.

It consists of two main sections: the upper section, which features window cutouts, and the lower section, which is windowless. These sections are joined using a custom-designed pair of 12" OD flanges. The upper section was initially utilized as a strand burner, as described in the work of Risha et al. The lower section was specifically added for this study to expand the chamber volume and enhance flow-through performance. An exhaust line was attached to the bottom of the lower section and directed outside the test cell.

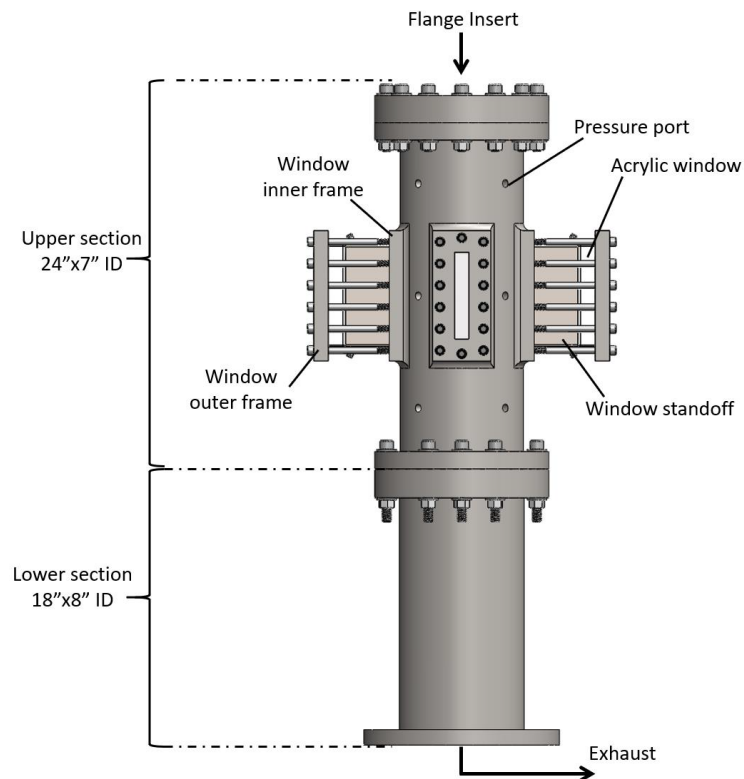


Figure 19. CAD model image of optically accessible combustion chamber with two modified window standoffs.

## Chamber Extension

The original chamber design, which included only the upper section, featured a flat bottom flange with a 1/4" exit hole. However, for this study, a larger volume and increased flow-through capacity were required to facilitate the exit of gas and solid combustion products.

To achieve this, a lower section was added to the chamber. Once fabricated, this section underwent hydrostatic pressure testing up to 500 psi. After successful testing, it was installed and securely connected to the bottom of the upper section, forming the expanded combustion chamber used in this research.

## Chamber Windows

A set of acrylic windows was utilized to provide optical access to the interior of the chamber. A dimensional model of the window pair is presented in Fig. 19.

The inner window, directly exposed to the chamber environment, had a thickness of 0.2" and was designed as a sacrificial component to be frequently replaced. It served to protect the thicker outer window while also ensuring a pressure seal by pressing against a face-sealed O-ring.

The outer window, with a thickness of 1", was designed to withstand elevated pressures, providing structural integrity during testing.

## Window Standoff and Purge System

Initial combustion tests revealed that within seconds of ignition, the chamber windows became obscured by combustion products, significantly limiting the duration of clear flame imaging. To mitigate this issue and extend the visibility period, a window "standoff" and purge flow system were introduced. These modifications were found to considerably improve the duration of unobstructed flame observation, depending on the operating conditions.

The design of the window standoff is illustrated in Fig. 20, while its impact on the chamber is depicted in Fig. 21. The standoff increased the distance that combustion byproducts needed to travel before accumulating on the window, thereby reducing contamination. Additionally, it created a cavity that enabled the introduction of a purge flow, further enhancing visibility during testing.

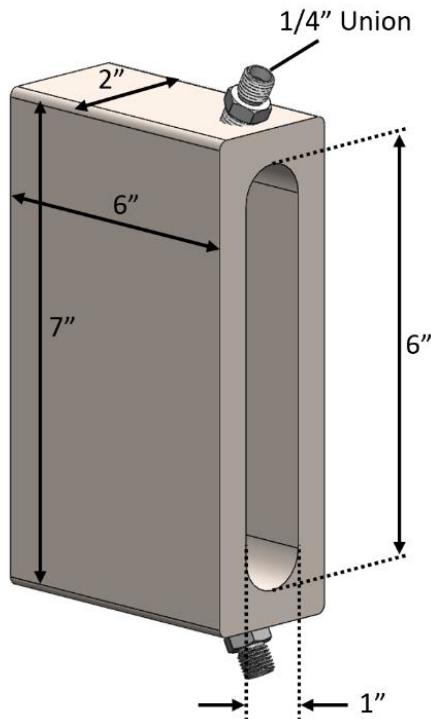
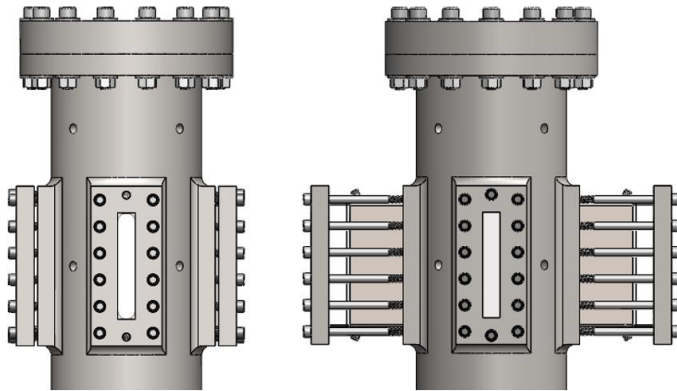


Figure 20. Combustion chamber window "standoff" CAD model image.



*Figure 21. Window section of combustion chamber with (right) and without (left) window standoffs.*

To facilitate the purge system, threaded holes were drilled at the top and bottom of the window standoff, where 1/4" Swagelok male unions were installed. Gas flows were directed into the standoff cavity through these fittings, as illustrated in Fig. 22 (left). These purge flows generated positive pressure and an outward flow within the standoff cavity, helping to prevent combustion byproducts from adhering to the window.

Additionally, within the chamber, a separate gas flow was introduced using an Exair 1" Flat Super Nozzle, forming a flat curtain flow over the entrance plane of the window cavity. As shown in Fig. 22 (right), this curtain flow further minimized the accumulation of combustion particles on the acrylic window.

The combination of standoff purge flow and curtain flow is referred to as the "shield flows." These protective flows were exclusively applied to the observation windows to ensure prolonged optical clarity during testing.

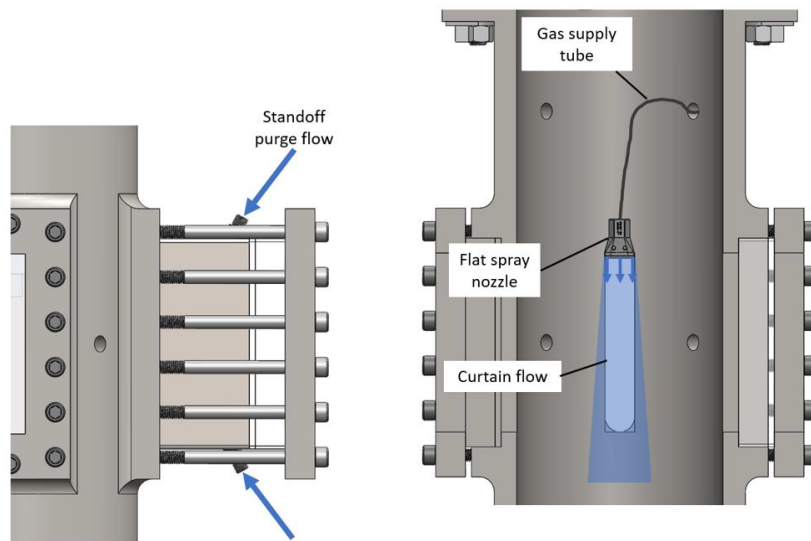


*Figure 22. Combustion chamber window standoff purge locations (left) and internal chamber view – window "curtain" flow (right).*

The combined use of the standoff purge flow and curtain flow provided a sufficient window of time (~2–10 seconds, depending on chamber pressure) to capture clear flame images.

To maintain a consistent environment within the chamber, the shield flows utilized the same gas as the combustion oxidizer. Each flow was supplied from a separate tank, and a choked orifice was installed on each line to regulate and maintain constant flow rates throughout the testing process.

## Control and Measurement Systems

Given the hazardous nature of pressurized combustion experiments, the system was operated remotely from a control room, which was physically separated from the test cell.

A primary computer running a LabVIEW VI was used to control the fluid system and acquire measurement data. In addition, a manual control box was available as an emergency override, allowing the system valves to be switched to a predetermined, hardwired state for safety.

For oxidizer flow control, a dedicated laptop located inside the test cell was used to operate the flow controller software. The high-speed Phantom v1212 camera was managed from a separate dedicated laptop in the control room.

During pressurized testing, a manual pressure regulator located in the control room was used to adjust the chamber pressure. Fig. 23 provides a detailed schematic of the control and measurement system components.

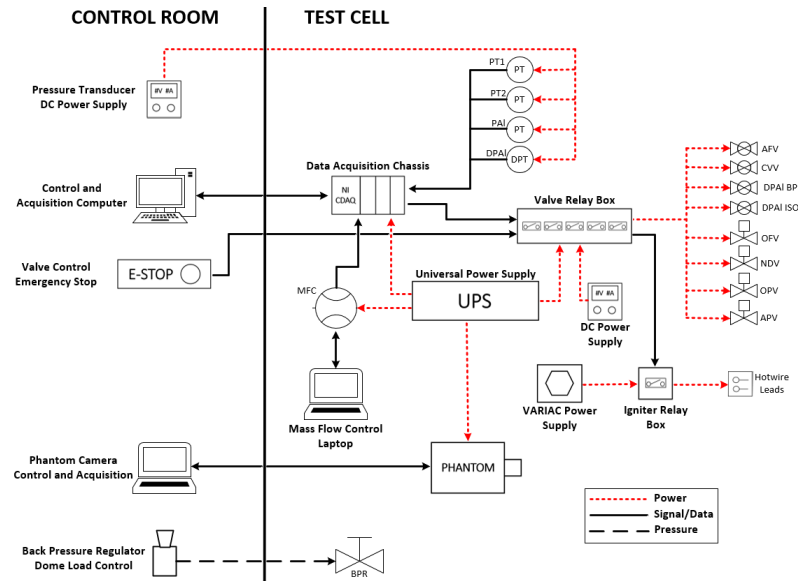


Figure 23. Control and data acquisition placement and connection diagram.

## Components and Instruments

1. **AFV (Argon Feed Valve)** - Pneumatically actuated ball valve.
2. **OFV (Oxidizer Flow Valve)** - Control valve for oxidizer.
3. **Swagelok 133 Series Pneumatic Actuator** - Used for driving ball valves.

4. **ASCO Redhat II Solenoid Valves** - Venting solenoid valves.
5. **Parker High-Pressure Rubber Hose** - Used for gas transportation.
6. **Swagelok Male Tube Fittings** - Connects tubing and gas lines.
7. **National Instruments cDAQ-9174 Chassis** - Data acquisition system.
8. **National Instruments LabVIEW VI** - Software used for control and data acquisition.
9. **Phantom v1212 High-Speed Camera** - Optical diagnostic tool.
10. **Teledyne Hastings HFC-D-303B Mass Flow Controller** - Used for oxidizer flow control.
11. **Setra Model 206 Pressure Transducers** - Measures chamber and fuel feed system pressures.
12. **Validyne P305D Differential Pressure Transducer** - Measures differential pressure across the fuel feed system.
13. **Praxair Type-T and Type-K Gas Cylinders** - Provides argon, nitrogen, and oxidizer gases.
14. **Equilibar GS4SNN1D Back Pressure Regulator** - Controls pressure in the chamber.
15. **TESCOM Manual Venting Regulator** - Used for setting back pressure regulator (BPR) levels.
16. **Bird Precision Choked Orifice** - Used to ensure constant flow rates.
17. **Swagelok Union Tee** - Part of the injector head.
18. **Nichrome Hotwire** - Used for ignition in the system.
19. **Conax Compression Fitting** - Seals and allows for high-pressure electrical feedthrough.
20. **Hydroxyl-Terminated Polybutadiene (HTPB) Solid Propellant** - Ignition material.
21. **PIV (Particle Image Velocimetry) System** - Measures turbulence and flow characteristics.
22. **Laser Quantum Opus 2W 532nm Laser** - Used in the PIV setup.
23. **Thorlabs BE10-532 10X Beam Expander** - Expands laser beams for imaging.
24. **Thorlabs 300mm Focal Length Plano-Convex Cylindrical Lens** - Used in laser sheet formation.
25. **Edmunds 532 ± 2nm Interference Filter** - Optical filter for PIV imaging.
26. **Nikon AF NIKKOR 50mm f/1.8 Lens** - Used with Phantom camera for capturing images.
27. **MKS Square Bandpass Filters** - Used in pyrometry diagnostics.

## Materials and Structural Components

1. **316L Stainless Steel** - Used for metal components.
2. **304 Stainless Steel** - Used for the combustion chamber.
3. **Buna-N Gaskets** - Used for sealing quick-clamp connections.
4. **ASTM 100 Mesh Sieve** - Used for filtering metal powder.
5. **Alloy Steel Bolts (Grade 8, 7/16"-14)** - Used for securing chamber windows.
6. **Acrylic Windows (0.2" and 1" thick)** - Used in combustion chamber optical access.
7. **Parker 2-251 O-ring** - Used for sealing flange insert.
8. **Exair 1" Flat Super Nozzle** - Used for window curtain flow.

## Software and Control Systems

1. **LabVIEW VI** - Software for controlling relays and acquiring measurement data.
2. **Phantom Camera Control (PCC) Software** - Used for controlling and acquiring images from the high-speed camera.
3. **LaVision DaVis Software** - Used for processing PIV images.
4. **MATLAB** - Used for image analysis and burning velocity calculations.

5. **PIVlab (Open Source Software)** - Used for processing particle image velocimetry data.

### ***"Investigation of Laminar Burning Velocity in Aluminum Particle Suspensions" (SEZER KOYUN)***

Understanding the burning behavior of particulate fuels is crucial for advancing combustion science, particularly for high-energy-density fuels like aluminum. This study focuses on measuring the laminar burning velocity of aluminum particle suspensions, a fundamental parameter that characterizes how flames propagate through a given fuel-oxidizer mixture. While the concept of laminar burning velocity is well established for gaseous and liquid fuels, its applicability to particulate fuels remains uncertain due to the complexities involved in particulate combustion.

Particulate combustion presents unique challenges that are not encountered in gaseous or liquid fuels. Factors such as particle inertia, radiative heat loss, heterogeneous reaction zones, and flow sensitivity significantly affect the burning process. These challenges make it difficult to obtain accurate and reproducible measurements of flame speed. By employing a counterflow flat-flame burner, this research aims to overcome these obstacles and provide a controlled environment for studying aluminum combustion. The study also compares its results with previous burning velocity measurements obtained from other methods, such as Bunsen burners, spherical flames, and propagating flames in tubes, to determine whether the concept of burning velocity can be reliably applied to aluminum particle suspensions.

### **Purpose and Objectives**

The primary objective of this study is to determine whether the concept of laminar burning velocity can be extended to particulate fuels like aluminum. To achieve this, the research is designed to accurately measure aluminum flame speeds under well-defined experimental conditions and compare them with values obtained using other combustion techniques.

Another key goal is to understand the effects of particle inertia, radiative heat loss, and particle distribution on the combustion process. Unlike gaseous flames, where fuel and oxidizer are homogeneously mixed, particulate combustion involves fuel particles dispersed in an oxidizing medium, leading to complex burning dynamics. The study seeks to address how these factors influence flame propagation and whether appropriate corrections can be applied to standard burning velocity models.

Additionally, the research aims to develop an improved methodology for measuring particulate burning velocity using high-speed imaging, particle tracking, and laser diagnostics. By integrating these advanced measurement techniques, the study aims to minimize uncertainties and provide a reliable framework for future investigations into particulate combustion.

### **Experimental Setup**

The experimental setup was carefully designed to stabilize aluminum flames in a counterflow burner system, allowing for precise measurements of burning velocity. This setup consists of several key components that ensure the stability and accuracy of the experiment.

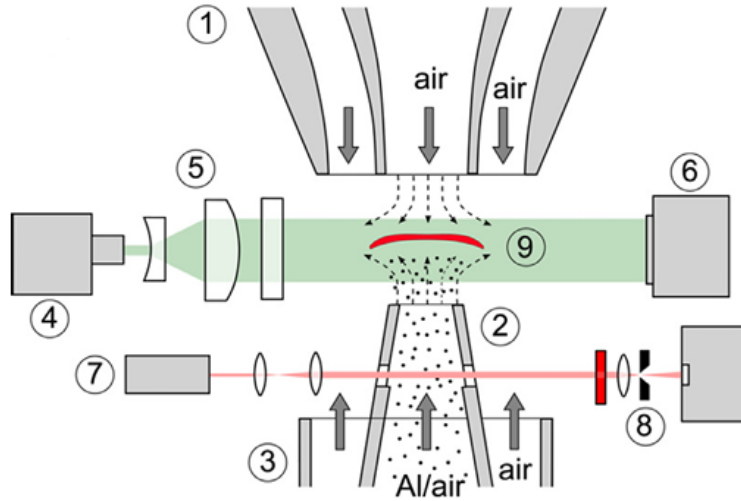


*Fig 24. (a) Counterflow apparatus and diagnostics. The numbered parts are (1) top nozzle with air co-flow, (2) bottom nozzle, (3) bottom co-flow, (4) 5 W green laser, (5) beam expansion optics, (6) Photron SA-5 high-speed camera, (7) 5 mW red laser, (8) photo-diode, (9) flat aluminum flame.*

A laminarizing tube (60 cm in length) was used to ensure that the aluminum-air suspension flowed smoothly before reaching the burner. The suspension exited through a bottom nozzle (1.5 cm in diameter), which directed the fuel-oxidizer mixture upward. A second, inverted nozzle was placed 2 cm above the bottom nozzle, creating a stagnation point where the aluminum flame stabilized. This counterflow configuration ensured that the flame was flat and well-defined, minimizing the effects of turbulence and allowing for accurate velocity measurements.

The fuel used in the experiment was Ampal 637 aluminum powder, with an average particle diameter of 5.6  $\mu\text{m}$ . The powder was hermetically stored to ensure consistent properties throughout the study, preventing unwanted oxidation and changes in particle distribution. This careful handling of fuel was essential to maintaining reproducibility and accuracy in the measurements.

### Instrumentation and Cost Considerations

To achieve precise measurements, the study employed advanced diagnostic tools designed for high-speed imaging, particle tracking, and flow analysis. These instruments included a high-speed camera, a 532 nm green laser system, Particle Image Velocimetry (PIV) software, a laser-light attenuation probe, and beam-shaping optics. Each instrument played a crucial role in capturing detailed images of flame structure and particle movement, ensuring accurate calculations of burning velocity.

The counterflow burner system itself was designed to provide a well-defined flat aluminum flame, creating a controlled and reproducible combustion environment. The careful selection of aluminum powder and real-time monitoring of dust concentration further ensured experimental consistency.

The total cost of the experimental setup, including all necessary equipment, software, and fuel, is estimated to range between \$100,000 and \$300,000. This estimate covers high-speed imaging technology, laser-based diagnostic tools, computational software, burner fabrication, and precision optical components. The price variation depends on factors such as equipment specifications, calibration needs, and whether second-hand or newly manufactured components were used.

## Results and Key Findings

The study successfully demonstrated that aluminum particle flames can be stabilized in a counterflow burner, allowing for the first-time direct measurement of laminar burning velocity in such systems. These results provide strong evidence that the burning velocity concept can be extended to particulate fuels when appropriate corrections are applied.

One of the most significant findings was that burning velocity measurements were largely independent of aluminum concentration within the tested range. This suggests that flame propagation in particulate suspensions follows distinct trends compared to gaseous flames, where burning velocity is highly dependent on mixture composition.

Additionally, the study addressed several critical challenges in particulate combustion. Particle inertia was found to be a key factor, as larger particles exhibited lag effects in flow measurements. Radiative heat loss was another major concern, as aluminum particles both absorb and emit heat differently than gases, influencing flame dynamics. By applying Stokes corrections to account for these effects, the researchers were able to obtain more accurate velocity profiles.

The comparison with previous Bunsen burner and spherical flame studies revealed that the counterflow burner technique provided more reliable burning velocity data due to its stable flame geometry and minimized heat loss.

## Conclusion

This study successfully demonstrated that laminar burning velocity can be applied to aluminum particle suspensions under controlled conditions. By stabilizing aluminum flames in a counterflow burner and employing state-of-the-art diagnostics, the researchers were able to obtain highly accurate burning velocity measurements, addressing long-standing challenges in particulate combustion.

The insights gained from this research have important implications for industries utilizing metal-based fuels, such as aerospace propulsion and advanced energy systems. The counterflow burner, combined with high-speed imaging and laser diagnostics, provides a robust platform for future studies into particulate combustion. Further work will be necessary to explore flame stretch, curvature effects, and hydrodynamic interactions, but this study lays the groundwork for improved efficiency and safety in particulate fuel applications..

### ***“Freely-Propagating Flames in Aluminum Dust Clouds” (ZEYNEP AKKUŞ)***

Metal particle suspensions in oxidizing environments are common in industries such as agriculture, propulsion, and energy production. Aluminum, among these metals, is particularly significant due to its use as an energetic additive in propellants, explosives, and pyrotechnics. Despite the

well-established research on hydrocarbon flames, the study of dust combustion remains underdeveloped, primarily due to the experimental challenges in maintaining uniform dust suspensions. Dust particles tend to settle quickly in quiescent environments, necessitating turbulent or microgravity conditions to achieve uniformity, complicating experimental setups. Additionally, dust combustion is highly influenced by particle morphology, size distribution, and system scale effects, making comparative analyses across studies challenging.

Traditional dust combustion studies often rely on closed vessel explosion tests that measure pressure rise to classify explosivity but provide limited insight into flame propagation dynamics. Recent advancements, however, have introduced techniques such as Bunsen-type stabilized flames and microgravity experiments. This study builds on systematic research at McGill University by introducing two experimental approaches to investigate freely propagating aluminum dust flames: (1) small-scale experiments with spherically expanding flames in transparent latex balloons and (2) large-scale unconfined aluminum dust cloud experiments in a fire tower. These setups aim to characterize flame propagation dynamics, identify instabilities, and explore the effects of turbulence and radiative heat transfer.

## Experimental Methods

### Small-Scale Flames in Balloons

The small-scale experiments employed transparent latex balloons, each with a diameter of 30 cm and an inflated volume of 14 L, to study spherically expanding aluminum dust flames under near-isobaric conditions. Aluminum powder was injected into the balloon using a pulsed high-pressure gas system to ensure uniform suspension, with ignition performed by a centrally positioned heated tungsten wire. A four-second delay was applied after dust injection to allow turbulence to subside before ignition. High-speed imaging at 4,000–7,500 fps recorded the dispersion dynamics, while laser light attenuation was used to measure dust concentration. Ampal 637 aluminum powder, known for its nodular morphology, was used due to its well-documented combustion characteristics.

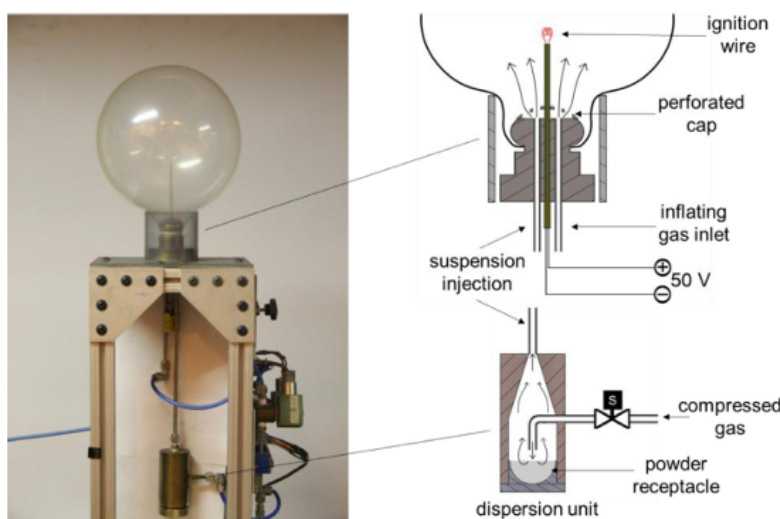


*Fig 25. Schematics and photograph of the laboratory apparatus for observation of spherical dust flames in transparent latex balloons.*

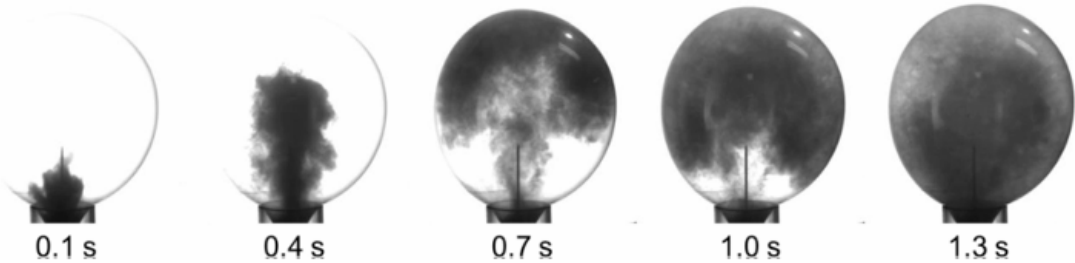


*Fig 26. Still frames of the dispersion of 4 g of aluminum powder in the latex balloon apparatus for a final concentration of approximately 200 g/m<sup>3</sup>*

### **Large-Scale Unconfined Flames**

The large-scale experiments were conducted in an indoor fire tower at the Fire Research Laboratory of Canada. A custom dust dispersal system created a 4 m tall, 2 m wide aluminum dust cloud by ejecting up to 1 kg of aluminum powder through a pneumatic piston and air-knife system. This process dispersed the dust uniformly within one second. A small 2 g black powder charge served as the ignition source, positioned at adjustable heights to control turbulence effects. Combustion dynamics were monitored using a grid of thermocouples to measure temperature history and a high-speed camera to capture flame propagation. The experiments utilized Valimet H-5 and H-10 aluminum powders with spherical morphology due to the large quantities required.

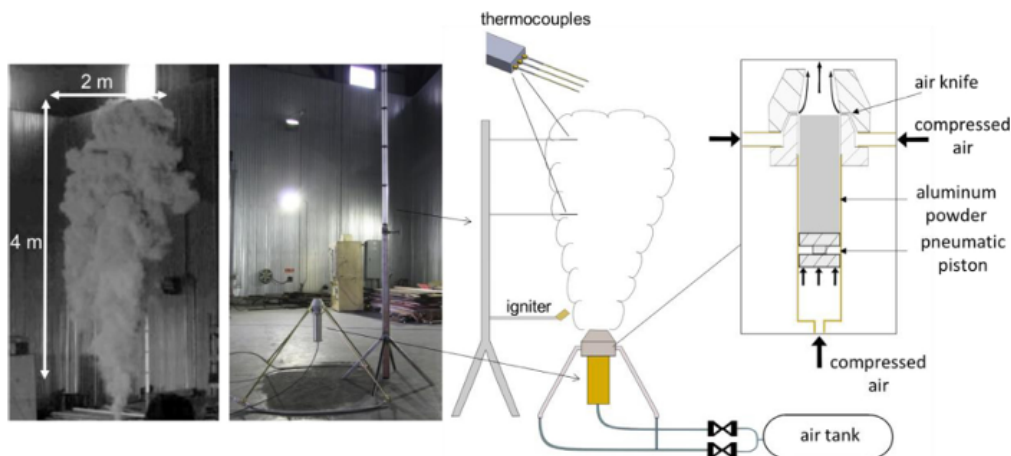


*Fig 27. Schematics ad photograph of the experimental rig for the large-scale dust cloud combustion tests*

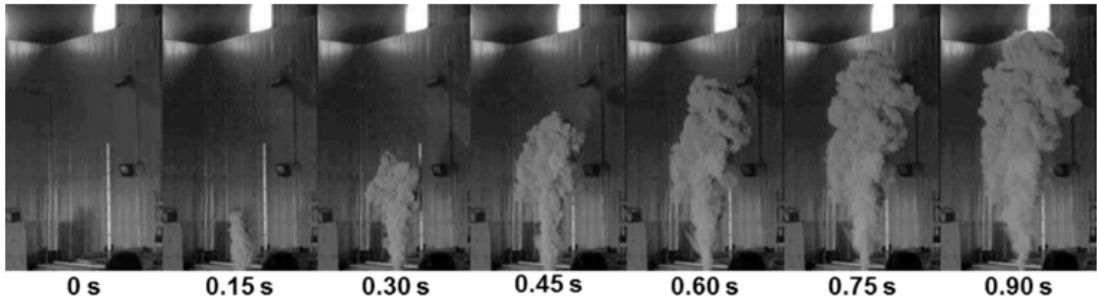


*Fig 28. Still frames of dust dispersion process for large-scale tests*

## Results

### Spherically Expanding Flames in Balloons

Multiple flame propagation regimes were observed during the small-scale experiments. Near stoichiometric aluminum concentrations, flames propagated smoothly and symmetrically outward from the ignition point. However, in fuel-lean mixtures, pulsating and spiral instabilities emerged, while fuel-rich mixtures exhibited cellular flame structures. Flame speed measurements showed that in fuel-lean conditions, the propagation speed was relatively insensitive to oxygen concentration, while in fuel-rich mixtures, increasing aluminum concentration had little effect on flame speed due to diffusion-limited combustion mechanisms.

### Large-Scale Flame Propagation Speeds

In the large-scale experiments, 18 trials were performed, and flame propagation was influenced by the level of turbulence in the dust cloud. Ignition delay times of 0.3–0.4 seconds significantly reduced turbulence effects, resulting in more consistent flame propagation. Flame speed measurements indicated that buoyancy forces contributed to observed flame motion. After correcting for buoyancy, the flame speeds showed good agreement with stoichiometric aluminum concentrations. The larger scale of these experiments allowed for significant radiative pre-heating, which enhanced flame propagation speeds compared to the small-scale experiments.

### Mixture Pre-Heating by Radiation

Thermocouple measurements in the large-scale experiments revealed a two-stage heating mechanism: pre-heating due to radiative flux from the flame and combustion products, followed by rapid molecular heating as the flame front arrived. This pre-heating was limited to 200°C and played a role in accelerating flame propagation without causing spontaneous ignition. The effects of radiation were negligible in small-scale experiments, as the scale was insufficient for effective absorption of radiative heat.

## Discussion

### Stable Flame Propagation

The burning velocity of spherically propagating dust flames was calculated by dividing the flame speed by the expansion coefficient, derived using NASA's CEA code. Burning velocities in

small-scale balloon experiments were consistent with prior Bunsen flame studies, but large-scale experiments showed nearly double the burning velocity. This increase was attributed to radiative pre-heating, which becomes significant only in larger clouds where self-absorption of radiation occurs.

### **Unstable Flames**

Pulsating and spiral instabilities observed in fuel-lean mixtures were linked to thermo-diffusive instabilities caused by imbalances between heat and mass diffusion. High Lewis numbers in fuel-lean conditions favored these instabilities, while cellular flame structures in fuel-rich mixtures were associated with low Lewis numbers. Unlike acoustic oscillations in gaseous flames, pulsating aluminum dust flames behaved like non-stationary thermal explosions, with periodic bursts of combustion energy driving propagation.

### **Conclusion**

This study provides a comprehensive dataset on freely-propagating aluminum dust flames under near-isobaric and unconfined conditions. Stable flame propagation occurred only near stoichiometric concentrations, while fuel-lean and fuel-rich mixtures exhibited pulsating, spiral, and cellular instabilities. Flame speed in fuel-lean mixtures was relatively insensitive to oxygen concentration, whereas in fuel-rich mixtures, increasing aluminum concentration had minimal impact due to diffusion-limited combustion mechanisms. Burning velocities were significantly higher in large-scale tests due to radiative pre-heating, a phenomenon absent in smaller flames. These findings contribute to the understanding of flame propagation dynamics in metal dust clouds and have implications for safety in industrial and propulsion applications.

### ***“Stabilized Flames in Hybrid Aluminum-Methane-Air Mixtures” (ZEYNEP AKKUŞ)***

This study examines stabilized flames in aluminum-seeded methane-air hybrid mixtures, focusing on the impact of aluminum particle concentration on combustion characteristics. Two-phase hybrid combustible mixtures, involving both solid and gaseous fuels, are widely present in industrial processes, coal combustion, material synthesis, and accidental explosions. While much prior research has focused on the combustion of large metal particles or solid propellants with low metal content, the behavior of micron and submicron-sized dense metal suspensions remains underexplored.

Recent studies suggest that extrapolating combustion models from large particles to smaller ones may be misleading due to a potential shift from a diffusion-limited to a kinetically-limited combustion regime. Additionally, most previous investigations relied on constant-pressure bomb tests, which provide limited insight into hybrid flame structure and propagation. While hybrid flame studies have been conducted on coal-methane systems, research on metal suspensions in gaseous flames remains scarce, apart from earlier work on boron-propane combustion.

This study provides new experimental evidence demonstrating the strong influence of aluminum particle concentration on hybrid combustion dynamics. Optical diagnostics, including spectroscopic measurements, are employed to analyze burning velocity, flame temperature, and aluminum combustion products. The findings confirm that aluminum significantly alters flame propagation behavior, and aluminum combustion in hybrid solid-gas systems must be understood as a frontal flame propagation phenomenon rather than a conventional diffusion-driven process. These

results provide valuable insights into metal-enhanced combustion applications, including solid propellants, pyrotechnics, and energetic materials.

## Experimental Apparatus

### Hybrid Flame Burner and Optical Diagnostics

The hybrid flame burner designed for this study incorporates several technical improvements from previous dust flame experiments, particularly in the dust dispersion system. It consists of a piston dust feeder combined with a "flow knife" disperser, ensuring controlled and continuous dispersion of aluminum particles into the flame. The premixed methane-air mixture is directed through a 40  $\mu\text{m}$  wide circular slot, forming a high-velocity jet that shears off and disperses aluminum dust from the advancing piston. Before reaching the nozzle, the flow passes through a conical diffuser and a 60 cm long supply tube, transforming initial turbulence into a laminar flow, allowing for stable hybrid flame formation.

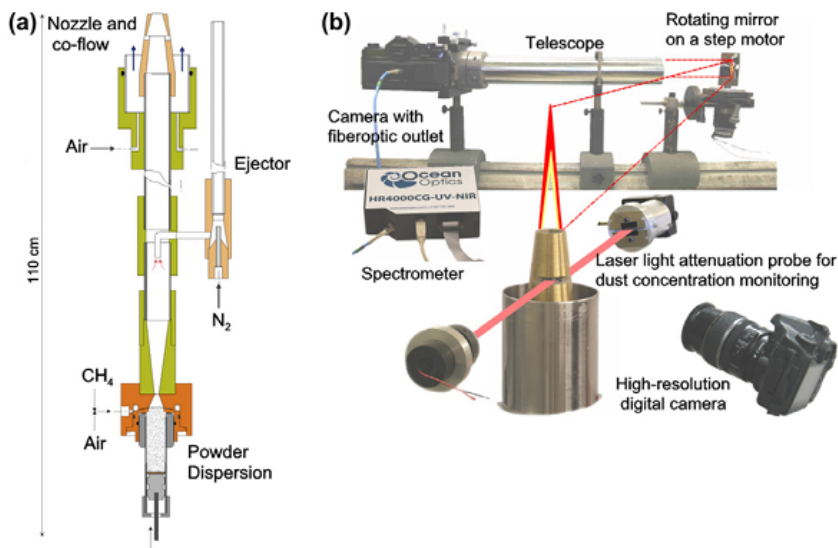


*Fig 29. Schematic of the hybrid flame burner and composite photograph of the optical diagnostic elements.*

The dust concentration in the flame is controlled by adjusting the speed of the piston and monitored using a laser light attenuation probe. This probe utilizes a 632 nm diode laser and a diode sensor with a narrow bandpass filter to measure dust concentration variations within the flow. To ensure precise calibration, dust is completely aspirated through a multi-layered filtration system with a vacuum pump, and the total dust mass is measured over a given time interval.

Flame visualization and combustion dynamics are captured using a high-resolution digital camera equipped with gray density filters to adjust image brightness. The camera's shutter release signals are synchronized with the dust concentration monitoring system for real-time correlation between dust dispersion and flame propagation.

For spectroscopic analysis, two spectrometers (Ocean Optics HR4000 CG-UV-NIR and USB4000) are employed. The HR4000 spectrometer, with a 5  $\mu\text{m}$  entrance slit and 0.6 mm fiber optic,

records high-resolution spectra (250–1000 nm, ~0.75 nm resolution), enabling the detection of AlO molecular bands and aluminum atomic lines. The USB4000 spectrometer, with a 0.1 mm fiber and no entrance slit, covers the 350–900 nm range (2.5 nm resolution) and is optimized for continuous flame temperature measurements. The HR4000 spectrometer provides detailed spectral features, while the USB4000 allows for high spatial resolution scanning (0.1 mm) with steps of 0.2–0.4 mm, ensuring accurate flame temperature distribution analysis.

This experimental setup enables precise control of hybrid aluminum-methane-air flames, facilitating an in-depth investigation of flame propagation, combustion characteristics, and spectral emissions.

## Experimental Results

### Flame Appearance, Spectra, and Temperature at Different Aluminum Concentrations

The aluminum–methane–air hybrid flames were studied at two different methane/air equivalence ratios: stoichiometric ( $\phi = 1$ ) and fuel-lean ( $\phi = 0.8$ ) conditions. Initially, a Bunsen-type conical flame was established at the nozzle exit without activating the dust dispersion system. However, even in the absence of active dust dispersion, the aluminum concentration remained above 20 g/m<sup>3</sup> due to surface erosion of compacted powder by the dispersing gas. To measure the pure methane–air flame speed, the system had to be completely emptied of aluminum powder.

Upon activating the piston-driven dispersion system, the aluminum concentration in the flow gradually increased until reaching a plateau. The total dispersion time varied between 3.5 to 6 minutes, with a maximum aluminum concentration ranging from 300 to 450 g/m<sup>3</sup>, depending on the piston speed.

Flame appearance changed significantly with increasing aluminum concentration. At low aluminum concentrations (< 50 g/m<sup>3</sup>), the flame exhibited a sharp inner boundary with an ill-defined outer boundary, appearing yellow in color. Individual particle streaks were visible under magnification. At higher aluminum concentrations (> 250 g/m<sup>3</sup>), the flames became bright-white and highly luminous, with a thin inner cone surrounded by a larger, well-defined diffusion flame.

The measured flame temperatures remained stable at ~1950 K for low aluminum concentrations but increased to 2750–2900 K for high aluminum concentrations (>250 g/m<sup>3</sup>).

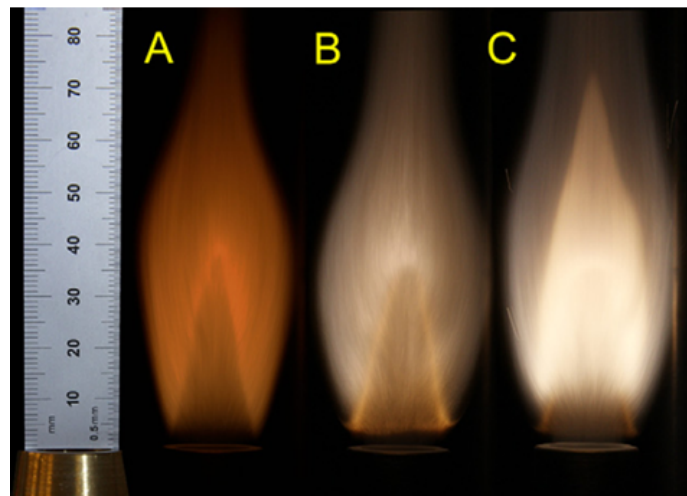


*Fig 30. Flame images at three different aluminum concentrations:(A)20–50g/m<sup>3</sup>, (B)140–200g/m<sup>3</sup>, and (C):250–400g/m<sup>3</sup>.*

### Burning Velocities of Aluminum–Methane–Air Hybrid Mixtures

The burning velocities of aluminum–methane–air hybrid mixtures were determined using the total flame surface area method, where the known volumetric flow rate through the nozzle was divided by the total surface area of the inner flame cone.

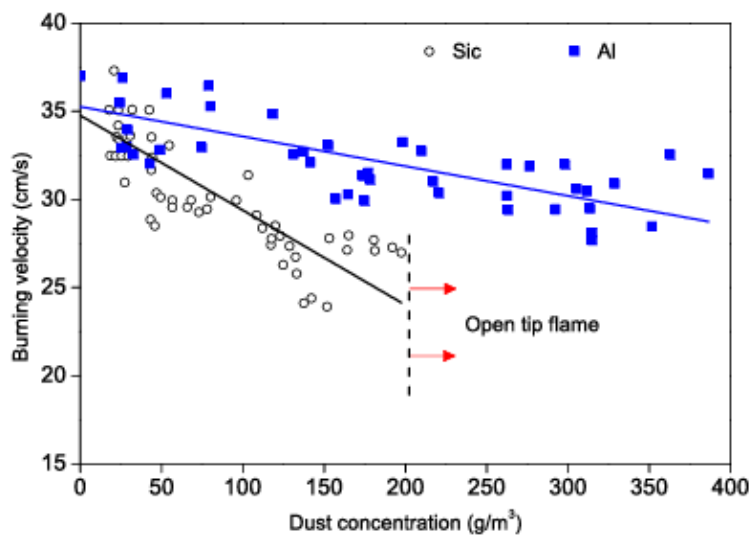


*Fig 31. Comparison of burning velocities in methane–air mixtures seeded with aluminum (Al) and silicon carbide (SiC) particles.*

Measured burning velocities for stoichiometric and lean methane–air hybrid mixtures indicate that flame burning velocity decreases only slightly with increasing dust concentration, suggesting that heat released by reacting aluminum enhances flame propagation.

To further analyze aluminum's role, additional tests were conducted using silicon carbide (SiC) particles of a similar size as an inert substitute for aluminum. The results show that flame burning velocity decreased significantly more with SiC than with aluminum. Despite aluminum

having a higher specific heat (0.90 J/g·K) than SiC (0.75 J/g·K) and requiring additional latent heat for melting, the flame remained more stable with aluminum.

At SiC concentrations above 200 g/m<sup>3</sup>, the flame began to destabilize, and at 300 g/m<sup>3</sup>, combustion was largely incomplete, with most of the fuel mixture escaping unburned. This result confirms that reacting aluminum particles contribute to the burning process, maintaining a higher flame propagation rate compared to inert dust particles.

### **3. Facility Summary**

#### **Single Particle Combustion**

To establish a metal particle combustion research facility, a range of specialized equipment is required to enable precise control and measurement of combustion processes. These instruments facilitate particle levitation, high-speed imaging, optical diagnostics, controlled ignition, and environmental regulation, ensuring reliable experimental conditions.

#### **Electrodynamic Levitator**

A key component of the facility is the electrodynamic levitator, which suspends a single aluminum particle in a gas mixture, isolating it from external convective influences. The system consists of top and bottom electrodes (80 mm in diameter) that generate an electric force to counteract gravity, ensuring vertical stability. A ring electrode with an AC voltage further stabilizes the particle laterally, allowing for precise control over its position. This setup is particularly useful for studying aluminum particles within the 20–100 μm range in a controlled environment, free from interference by supports or neighboring particles.

#### **High-Speed Imaging and Optical Diagnostics**

To analyze combustion dynamics, high-speed imaging is critical. The Phantom v1212 High-Speed Camera, with an operational speed of 4 kHz to 18 kHz, captures rapid changes in the burning process. Equipped with RGB matrices, it measures light intensity at three distinct wavelengths (450 nm, 530 nm, and 630 nm), enabling detailed optical analysis. This imaging system plays a crucial role in understanding combustion behavior by tracking burning time, ignition delay, and particle fragmentation.

For detailed imaging, the Questar QM 100 Teleobjective Lens provides high-resolution magnification, ensuring precise measurements of particle size and alumina residue formation. The optical setup minimizes interference from flame emissions and captures the light intensity at different wavelengths, aiding in spectral analysis.

#### **Light Source and Spectroscopic Analysis**

A white LED backlight (SOLIS-3C) is used to measure light absorption by alumina particles at multiple wavelengths, allowing for accurate size and concentration analysis. A multispectral light attenuation method is employed, leveraging absorption variations at 450 nm, 530 nm, and 630 nm to infer particle size and distribution profiles.

To complement these measurements, two spectrometers are utilized. The Ocean Optics HR4000 CG-UV-NIR Spectrometer records high-resolution spectra in the 250–1000 nm range, allowing the detection of AlO molecular bands and aluminum atomic lines. The USB4000 Spectrometer, optimized for flame temperature measurement, provides continuous spectra in the 350–900 nm range, ensuring high spatial resolution scanning.

### **Ignition and Combustion Control**

A CO<sub>2</sub> laser ignition system provides a non-contact, high-precision ignition source for aluminum particles. The 20 W CO<sub>2</sub> laser focuses symmetrically on the particle, ensuring uniform heating and preventing displacement due to thermophoretic forces. This is crucial for maintaining precision in combustion studies, as any external force can affect the particle's behavior.

### **Gas and Pressure Control Systems**

The combustion environment is carefully regulated using a controlled gas mixture chamber, allowing precise adjustments of CO<sub>2</sub>, CO, N<sub>2</sub>, and H<sub>2</sub>O mixtures. A steam supply system further enhances experimental flexibility by introducing water vapor into the combustion process, enabling studies on H<sub>2</sub>O/CO<sub>2</sub> and H<sub>2</sub>O/O<sub>2</sub> mixtures.

A pressure regulation system maintains stable experimental conditions, with capabilities up to 15 atm. This ensures consistent combustion conditions and reliable data acquisition. To monitor gas composition during combustion, a Horiba PG-250 Gas Analyzer tracks emissions such as CO<sub>2</sub>, O<sub>2</sub>, and NO<sub>x</sub>, providing insights into combustion efficiency and chemical byproducts.

### **High-Pressure Combustion Chamber**

The high-pressure combustion chamber simulates extreme conditions found in solid rocket motors and industrial processes. Made from a high-strength aluminum alloy, it withstands pressures of up to 8 MPa and measures 100 mm in diameter and 200 mm in length. This chamber features optical access windows made from Zn-Se and quartz, allowing both visible and infrared diagnostics.

### **Experimental Measurements and Data Acquisition**

Several key experimental parameters are measured using this setup:

- Burning Time: Synchronized high-speed imaging and photomultiplier tubes (PMTs) are used to measure the duration of combustion.
- Ignition Delay: Defined as the time from laser heating to particle ignition, this measurement assesses how particle properties and environmental conditions influence reactivity.
- Particle Size Analysis: Using calibrated imaging tools, the diameter of aluminum particles before and after combustion is measured, providing insights into combustion efficiency and residue formation.

## **Cost and Availability Considerations**

The establishment of this facility requires careful planning and budgeting due to the high cost and limited availability of certain equipment. The Phantom v1212 High-Speed Camera alone exceeds \$100,000, while the PIV (Particle Image Velocimetry) System costs over \$50,000. Other essential components, such as the Laser Quantum Opus 2W 532nm Laser (\$10,000 – \$20,000) and the Teledyne Hastings HFC-D-303B Mass Flow Controller (\$2,000 – \$5,000), are not readily available in Turkey. Some instruments, including the National Instruments cDAQ-9174 Chassis (\$1,500 – \$3,000) and the Swagelok 133 Series Pneumatic Actuator (\$500 – \$1,000), have limited availability but can still be sourced domestically with strategic supplier partnerships.

Given the high costs and procurement challenges, international sourcing will be required for most of the critical high-speed imaging and laser diagnostic equipment. The facility's success depends on careful integration of these advanced systems to ensure precise control of combustion conditions, reliable data acquisition, and repeatable experiments under controlled pressure and gas mixtures.

This facility, when fully equipped, will enable cutting-edge research in metal particle combustion, contributing to advancements in solid propellants, industrial safety, and energy applications.

## **Metal Dust Combustion**

### **High-Speed Imaging and Optical Analysis**

A crucial addition to the facility is the Phantom v1212 High-Speed Camera, priced at \$100,000+, which provides extremely high frame rates necessary for capturing rapid combustion events. This system complements the previously discussed high-speed imaging setup by offering enhanced resolution and dynamic range, essential for tracking particle ignition, flame propagation, and combustion instabilities.

For particle tracking and velocity measurement, a Particle Image Velocimetry (PIV) System, costing \$50,000+, is integrated. This system utilizes laser illumination and high-speed cameras to measure the velocity fields of burning particles, aiding in the detailed analysis of metal dust combustion dynamics.

### **Laser and Spectroscopic Diagnostics**

To support optical diagnostics, the Laser Quantum Opus 2W 532nm Laser (\$10,000 – \$20,000) is incorporated for precise laser-based measurement techniques. This laser is critical for illuminating dust clouds and metal particles, allowing for accurate combustion analysis via scattering and absorption methods.

A Thorlabs BE10-532 10X Beam Expander (\$1,000 – \$2,000) is added to enhance the laser's beam profile, ensuring uniform illumination for experiments requiring high-precision optical measurement.

### **Flow and Pressure Control Systems**

To maintain stable combustion conditions, precise flow regulation components are included. The National Instruments cDAQ-9174 Chassis (\$1,500 – \$3,000) is essential for data acquisition and

control, enabling seamless integration of various sensors monitoring pressure, temperature, and gas composition.

The Teledyne Hastings HFC-D-303B Mass Flow Controller (\$2,000 – \$5,000) is added to regulate gas mixtures and flow rates, ensuring consistent experimental conditions in the combustion chamber.

For **pressure control**, the facility includes:

- Equilibar GS4SNN1D Back Pressure Regulator (\$1,000 – \$2,500), maintaining precise control over gas pressure in the combustion chamber.
- TESCOM Manual Venting Regulator (\$500 – \$1,500), allowing for manual adjustments of gas flow.
- Swagelok 133 Series Pneumatic Actuator (\$500 – \$1,000), providing automated control over flow systems.

These additions significantly improve the facility's capabilities in metal particle combustion research, ensuring precise control over flow dynamics, imaging, and combustion diagnostics. Integrating these components into the existing setup enhances experimental accuracy, repeatability, and the ability to study complex combustion phenomena in detail.

## References

- Peng, F., Liu, H., & Cai, W. (2023). Combustion diagnostics of metal particles: a review. *Measurement Science and Technology*, 34(4), 042002.  
<https://doi.org/10.1088/1361-6501/acb076>
- Shafirovich, E., & Varma, A. (2008). Metal-CO<sub>2</sub> propulsion for Mars missions: current status and opportunities. *Journal of Propulsion and Power*, 24(3), 385–394.  
<https://doi.org/10.2514/1.32635>
- Foster, G., Kempema, N., Boyer, J., Harris, J., & Yetter, R. (2022). Experimental investigation of aluminum-air burning velocity at elevated pressure. *Combustion and Flame*, 248, 112532.  
<https://doi.org/10.1016/j.combustflame.2022.112532>
- Keck, H., Chauveau, C., Legros, G., Gallier, S., & Halter, F. (2024). New experimental method for the simultaneous determination of concentration and size profiles of condensed combustion products around a burning aluminum droplet. *Combustion and Flame*, 268, 113616. <https://doi.org/10.1016/j.combustflame.2024.113616>
- Julien, P., Whiteley, S., Soo, M., Goroshin, S., Frost, D. L., & Bergthorson, J. M. (2016). Flame speed measurements in aluminum suspensions using a counterflow burner. *Proceedings of the Combustion Institute*, 36(2), 2291–2298. <https://doi.org/10.1016/j.proci.2016.06.150>
- Legrand, B., Marion, M., Chauveau, C., Gokalp, I., & Shafirovich, E. (2001). Ignition and combustion of levitated magnesium and aluminum particles in carbon dioxide. *Combustion Science and Technology*, 165(1), 151–174. <https://doi.org/10.1080/00102200108935830>
- Marion, M., Chauveau, C., & Gökalp, I. (1996). Studies on the ignition and burning of levitated aluminum particles\*. *Combustion Science and Technology*, 115(4–6), 369–390.  
<https://doi.org/10.1080/00102209608935537>
- *Electromagnetic levitator.* (n.d.).  
[https://www.esa.int/Science\\_Exploration/Human\\_and\\_Robotic\\_Exploration/Blue\\_dot/Electro\\_magnetic\\_levitator](https://www.esa.int/Science_Exploration/Human_and_Robotic_Exploration/Blue_dot/Electro_magnetic_levitator)

- Julien, P., Vickery, J., Goroshin, S., Frost, D. L., & Bergthorson, J. M. (2015). Freely-propagating flames in aluminum dust clouds. *Combustion and Flame*, 162(11), 4241–4253. <https://doi.org/10.1016/j.combustflame.2015.07.046>
- Soo, M., Julien, P., Goroshin, S., Bergthorson, J. M., & Frost, D. L. (2012). Stabilized flames in hybrid aluminum-methane-air mixtures. *Proceedings of the Combustion Institute*, 34(2), 2213–2220. <https://doi.org/10.1016/j.proci.2012.05.044>
- *Solid Combustion Experiment Module (SCEM) | JAXA Human Spaceflight Technology Directorate.* (n.d.). JAXA Human Spaceflight Technology Directorate.  
<https://humans-in-space.jaxa.jp/en/biz-lab/experiment/facility/pm/scem/?utm>
- *Engine combustion.* (n.d.). Combustion Research Facility.  
<https://crf.sandia.gov/research/engine-combustion/>
- **Papike, J. J., Simon, S. B., & Laul, J. C. (1982).** "The lunar regolith: Chemistry, mineralogy, and petrology." *Reviews of Geophysics*, 20(4), 761-826.